

# Representation of seasonal land-use dynamics in SWAT+ for improved assessment of blue and green water consumption

Anna Msigwa<sup>1,2</sup>, Celray James Chawanda<sup>2</sup>, Hans C. Komakech<sup>1</sup>, Albert Nkwasa<sup>2</sup>, and Ann van Griensven<sup>2,3</sup>

5 <sup>1</sup>The Nelson Mandela African Institution of Science and Technology, Arusha 447, Tanzania

2 Department of Hydrology and Hydraulic Engineering, Vrije Universiteit, Pleinlaan 2 -1050, 1050 Brussel, Belgium

3 IHE-Delft Institute for Water Education; Westvest 7, 2611 AX Delft, The Netherlands

Correspondence to: Anna Msigwa (anna.msigwa@nm-aist.ac.tz)

**Abstract.** In most (sub)-tropical African cultivated regions, more than one ~~cropping cycle~~cropping season exists following the (one or two) rainy seasons. During the dry season, an additional ~~cropping cycle~~cropping season is possible when irrigation is applied, which could result in 3 cropping seasons. ~~However, most studies for mapping the blue and green water ET with agro-hydrological models such as SWAT do not better represent these cropping seasons~~In most agro-hydrological model applications such as SWAT+ in Africa, only one cropping season per year is represented. Blue ET is a portion of crop evapotranspiration after application of irrigation while green ET is the evapotranspiration as a result of rainfall. In this paper, we derived dynamic and static trajectories from seasonal land-use maps to represent the land-use dynamics following the major growing seasons, for the purpose of improving simulated— blue and green water consumption from simulated evapotranspiration (ET) in SWAT+. ~~This study builds upon earlier research that proposed an approach on how to incorporate seasonal land use dynamics in the SWAT+ model but mainly focused on the temporal pattern of LAI and tested the approach in a small catchment (240 km<sup>2</sup>). Together with information obtained from the cropping calendar, we implemented agricultural management operations for the dominant trajectory of each agricultural land-use class for the Kikuletwa basin (6650 km<sup>2</sup> area coverage) in Tanzania.~~ A comparison between the default SWAT+ (with static land use representation) set up, and a dynamic SWAT+ model (with seasonal land use representation) is done by spatial mapping of the evapotranspiration (ET) results. ~~Moreover~~Additionally, the SWAT+ blue and green ET were compared with the results from the four remote sensing data-based methods namely: SN (Senay et al., 2016), EK (van Eekelen et al., 2015), Budyko method and Soil Water Balance method (SWB). The results show that ET with seasonal representation is closer to remote sensing ~~estimation~~estimates, giving higher performance ~~than ET with static land use representation~~than default: ~~T~~he Root Mean Squared Error decreased from 181 to 69 mm/year; the percent bias decreased from 20 % to 13% and Nash Sutcliffe Efficiency increased from -0.46 to 0.4. ~~Further~~ ~~It is concluded that representation of seasonal land use dynamics produces better ET results which provide better estimations of blue and green agricultural water consumption.~~ ~~T~~he results of blue and green ET from the dynamic SWAT+ model ~~as were~~ compared to the four remote sensing methods. ~~The results further shows that the SWAT+ blue and green ET are similar to the van Eekelen method that performed better than~~the other three remote sensing methods. ~~I~~ts concluded that representation of

seasonal land-use dynamics produces better ET results which provide better estimations of blue and green agricultural water consumption.

## 1. Introduction

35 Freshwater availability will become is a limiteded resource in many regions throughout the world and the problem is projected to increase in the near future due to the increasing risks of land use change, population growth, and climate change. The availability of freshwater is mostly determined by precipitation on land. When rain falls on land, it travels via either green or blue waterways (Velpuri and Senay, 2017; Hoekstra, 2019). The green water resource is the water that is held in the unsaturated soil  
40 layer, whereas the blue water resource is the water that is stored in rivers, streams, surface-water bodies, and groundwater (Falkenmark and Rockström, 2006). One of the solutions to lessen the threat of freshwater scarcity is to minimize consumptive water use in agriculture. However, for water resource management, it is critical to understand water use in agricultural production by source (rainwater or irrigation water from surface and groundwater) (Velpuri and Senay, 2017). For efficient water resource  
45 management, knowing how much direct rainwater (green water) and non-rainwaterabstracted water (blue water) is being utilized for irrigation is crucial. Yet such information is not readily available, especially forin developing countries.

Hydrological models such as the Soil Water Assessment Tool (SWAT) arecan be used to provide information on blue and green water onat a-basin and continental scales (Xie et al., 2020; Jeyrani et al., 50 Liang et al., 2020; Serur, 2020). For instance, (Schuol et al., (2008) used the SWAT model to simulate blue and green water availability for the African continent. to (Xie et al., (2020), evaluated the evolution of the blue and green water resources, water footprints, and water scarcities in time and space in the Yellow River basin in China from 2010–2018. The study accounts for the effects of irrigation on blue and green water resources. (Liang et al., (2020) used the SWAT model combined with future land  
55 use and climate scenarios, which was successfully applied to quantify the spatiotemporal distribution of blue and green water change for the Xiangjiang River Basin in China between 2015 and 2050.

However, a few of these studies have implemented annual land-use dynamics. Since land-use refers to manmade socio-economic activities and management practices on the land, these anthropogenic activities may change depending on a season, specifically on cultivated land (Anderson et al., 1976). These changes per season are called seasonal land-use dynamics (Msigwa et al., 2019). Hence, mapping the blue and green water with agro-hydrological models such as SWAT need a better representation of the seasonality/cropping seasons. To best of our knowledge there are no studies~~s~~ that implemented seasonal land-use dynamics in estimation of blue and green water resources. For example, Jeyran et al. (2021), assessed basin blue and green available water components under different management and climatic scenario using SWAT. The annual land-use ~~dynamic~~ change implementation showed that the 30% increase in agricultural land use from 1987 to 2015 has caused significant changes in water shortages of Tashk-Bakhtegan basin in Iran. However, other studies do not implement even the annual land-use dynamic in order to decrease the computational time of the very large-scale models. In most cases, the dominant soil and land cover are used. For instance, (Serur, 2020) used a 10-year land use map to model blue and green water availability for the Weyb River basin in Ethiopia.

The major problem with the previous limitation of applying these approaches is that in the Tropical African cultivated areas is typically that typically they have more than one growing cycle, most of the time ranging between 2 to 3 depending on the sequence of rainy and dry seasons and availability of irrigation water (Msigwa et al., 2019). The right representation and timing of these cropping seasons is therefore important in order to quantify the crop water consumption.

A FA Representation of land-use dynamics in agro hydrological models is important due to the numerous impacts of land-use changes on water resources. LULC changes affect hydrologic processes such as infiltration, groundwater recharge, evapotranspiration, and runoff (Welde and Gebremariam, 2017; Liu et al., 2008; Schilling et al., 2010). Several studies have demonstrated the importance of incorporating dynamic land-use change in models (Chiang et al., 2010; Wagner et al., 2016). For instance, Wagner et al., (2016) found a continuous decrease of annual evapotranspiration of up to 53mm (7%) when dynamic land-use change is implemented per sub-basin scale.

However, most of these studies have implemented annual land use dynamic. Since land use refers to manmade socio-economic activities and management practices on the land, these anthropogenic activities may change depending on a season, specifically on cultivated land (Anderson et al., 1976). These changes per season are called seasonal land use dynamics (Msigwa et al., 2019). Few studies that have implemented seasonal land-use dynamic for other purposes such as nitrogen leaching and plant growth (Glavan et al., 2015), when estimating water withdrawals (Msigwa et al., 2019) and Leaf Area Index (LAI) simulation (Nkwasa et al., 2020), have found an impact of representing seasonal land-use dynamics in models. For instance, Nkwasa et al. (2020) found that the implementation of seasonal land-use dynamics in SWAT and SWAT+ models led to an improved vegetation simulation. The LAI dynamics of the seasonal land-use dynamic implementation showed more realistic temporal advancement patterns that corresponded to the seasonal rainfall within the basin. Moreover, Msigwa et al. (2019) found that water withdrawals for irrigated mixed crops increased by 482 Mm<sup>3</sup>/year when seasonal land-use maps are used. On the other hand, the seasonal land use-dynamics have been studied and evaluated using four methods that use multi-scalar datasets to assess cropping intensity of smallholder farms. In this study, the cropping intensity is the number of crops planted annually (Jain et al., 2013). However, in this case, the impact of seasonal land use on water resources has not been studied. Also, the implementation of seasonal land-use dynamic in SWAT and SWAT+ models led to an improved vegetation simulation (Nkwasa et al., 2020). The LAI dynamics of the seasonal land-use dynamic implementation showed more realistic temporal advancement patterns that corresponded to the seasonal rainfall within the basin.

The SWAT model incorporates crop rotation and its management at the level of the Hydrological Response Unit (HRU) within a sub-basin (Neitsch et al., 2002). It is represented as a sequence of planting and harvesting operations within the same HRU supplemented with management operations (Gao et al., 2017). The representation of agricultural management is done through a separate management file by specifying the planting, harvesting, tillage, irrigation, fertilizer and pesticide application by heat units or month and date (Arnold et al., 2018). Although, the SWAT (+) model is capable of representing multiple cropping seasons, however this is mainly implemented outside Africa catchments. Agro-hydrological model applications in Africa basins do typically not represent different cropping seasons. Rather

110 implement the default SWAT simulation of a single growing cycle every year (Ndomba et al., 2008; Koch et al., 2012; Gashaw et al., 2018). Lack of consideration of the seasonal land-use dynamics in hydrologic modelling studies, especially in African cultivated basins, may be attributed to past constraints of model capabilities, as well as lack of availability of crop-specific and agricultural management practices data (van Griensven et al., 2012).

115 Hence, the crop-specific and data management practices could be obtained from the seasonal land use maps using trajectory analysis. There has been a lot of improvement in how to represent the management operations by utilizing decision tables in the SWAT+ model, which is the revised and improved version of SWAT (Arnold et al., 2018; Bieger et al., 2017). In hydrological models, such as SWAT, the seasonal land-use dynamics could be implemented using trajectory analysis. Nkwasa et al., (2020) implemented  
120 seasonal land-use dynamic in SWAT and SWAT+ through land use trajectories, and not land cover classes. Trajectories represent changes of land-use over time by comparing changes between two or several land-use maps at a grid scale. Trajectory analysis has been applied widely to assess the changes and impact of Land Use and Land Cover (LULC) (Feng et al., 2014; Wang et al., 2012), and as a pre-processing tool for LULC (Zomlot et al., 2017). In these studies, change analysis is done pixel by pixel  
125 for each year in order to identify land use change (Mertens and Lambin, 2000; Swetnam, 2007; Zhou et al., 2008; Wang et al., 2012; Zomlot et al., 2017). However, none of these studies have analysed pixel by pixel within a year with the aim of identifying the different (cropping) seasons, further referred to as land use dynamics.

130 Tropical African cultivated areas typically have more than one growing cycle, most of the time ranging between 2 to 3 depending on the sequence of rainy and dry seasons and availability of irrigation water (Msigwa et al., 2019). The right representation and timing of these cropping seasons is important in order to quantify the crop water consumption. Agro-hydrological model applications in Africa basins do typically not represent different cropping seasons (Ndomba et al., 2008; Koch et al., 2012; Gashaw et al., 2018). Lack of consideration of the seasonal land-use dynamics in hydrologic modelling studies, especially in African cultivated basins, may be attributed to past constraints of model capabilities, as well  
135

as lack of availability of crop specific and agricultural management practices data (Van Griensven et al., 2012).

The SWAT model incorporates crop rotation and its management at the level of the Hydrological Response Unit (HRU) within a sub basin (Neitsch et al., 2002). It is represented as a sequence of planting and harvesting operations within the same HRU supplemented with management operations (Gao et al., 2017). The representation of agricultural management is done through a separate management file by specifying the planting, harvesting, tillage, irrigation, fertilizer and pesticide application by heat units or month and date (Arnold et al., 2018). There has been a lot of improvement in how to represent the management operations by utilizing decision tables in the SWAT+ model, which is the revised and improved version of SWAT (Arnold et al., 2018; Bieger et al., 2017). A recent study by Nkwasa et al., (2020) in the Usa catchment with in Kikuletwa basin in northern Tanzania has shown how to represent seasonal land-use dynamics using trajectories in the SWAT model using the management file and the SWAT+ model using decision tables for accurate hydrological simulation. Although the SWAT (+) model is capable of representing multiple cropping seasons, this is rarely implemented. By default, SWAT simulates a single growing cycle every year. There is increasing availability of satellite imagery suitable for land use monitoring with high resolution e.g. Landsat (up to 30m) (Belton et al., 2020; Al Hamdan et al., 2017) or Sentinel mission of the European Space Agency (ESA) (up to 5m) (Bergsma and Almar, 2020; Drusch et al., 2012; Berger et al., 2012). After further analysis, these images provide frequent land-use information such as crop types, cropping rotations and irrigation seasons even for small scale agricultural areas in African basins.

This paper builds from previous work that proposed an approach on how to incorporate seasonal land use dynamics in SWAT and SWAT+ models but was only evaluated for the temporal pattern of LAI simulations at a small catchment of 240 km<sup>2</sup> (Nkwasa et al., 2020). This study builds on the Nkwasa et al. (2020)'s approach aims to evaluate the effects of seasonal land-use dynamics on blue and green evapotranspiration ET, with two main objectives; (i) investigate the effect of implementing seasonal land-use dynamics on the water balance component in Kikuletwa basin (6650 km<sup>2</sup>) with focus on the ET using SWAT+ and (ii) to estimate blue and green water consumption from simulated ET. Seasonal land-

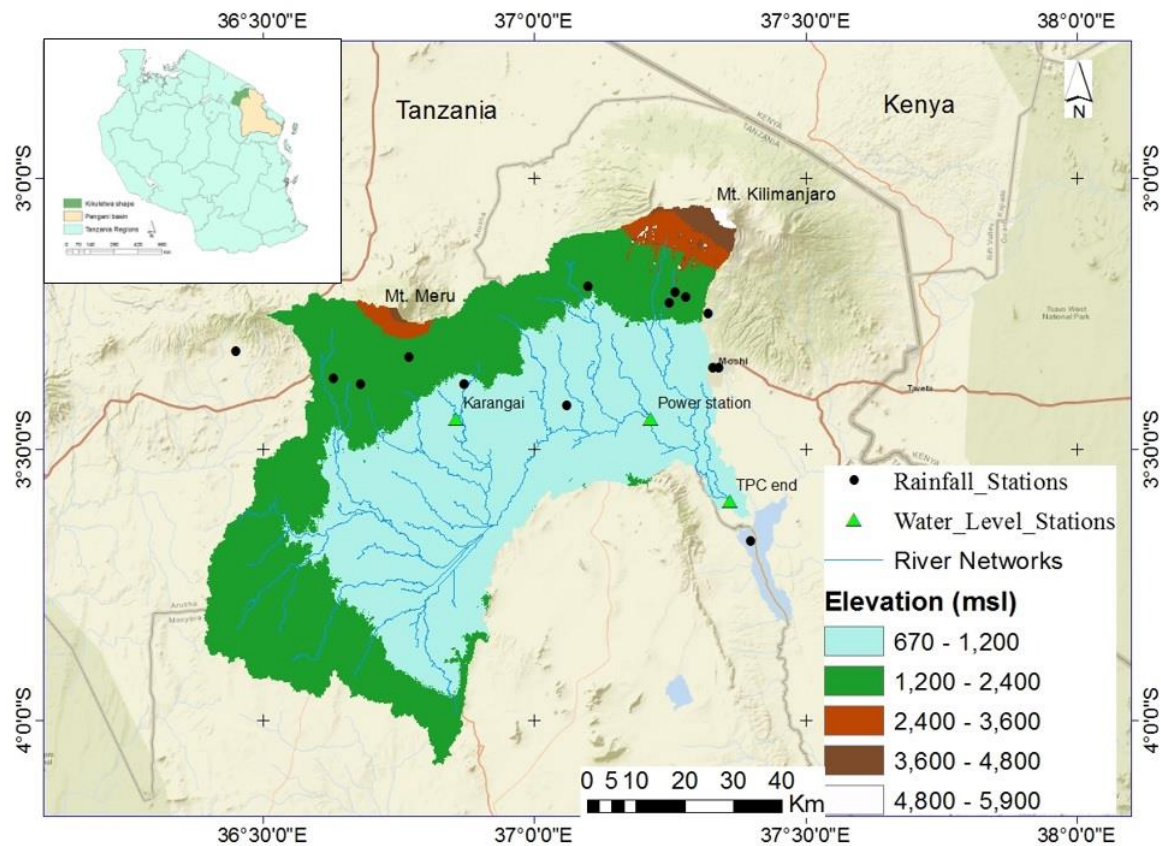
use maps were obtained from remote sensing to derive dynamic and static trajectories at 30m resolution (Msigwa et al., 2019). Together with information obtained from the cropping calendar, we implemented 165 agricultural operations for the dominant dynamic trajectory of each land use class using the approach proposed by Nkwasa et al., (2020). The paper compares spatial mapping of ET obtained from the default SWAT+ model set up with a static land use map and a SWAT+ model set up with seasonal dynamic land use representation. Findings from this study are intended to enhance the understanding of the spatial 170 temporal variability of water consumption (e.g. expressed as blue and green water uses) through improved ET estimations.

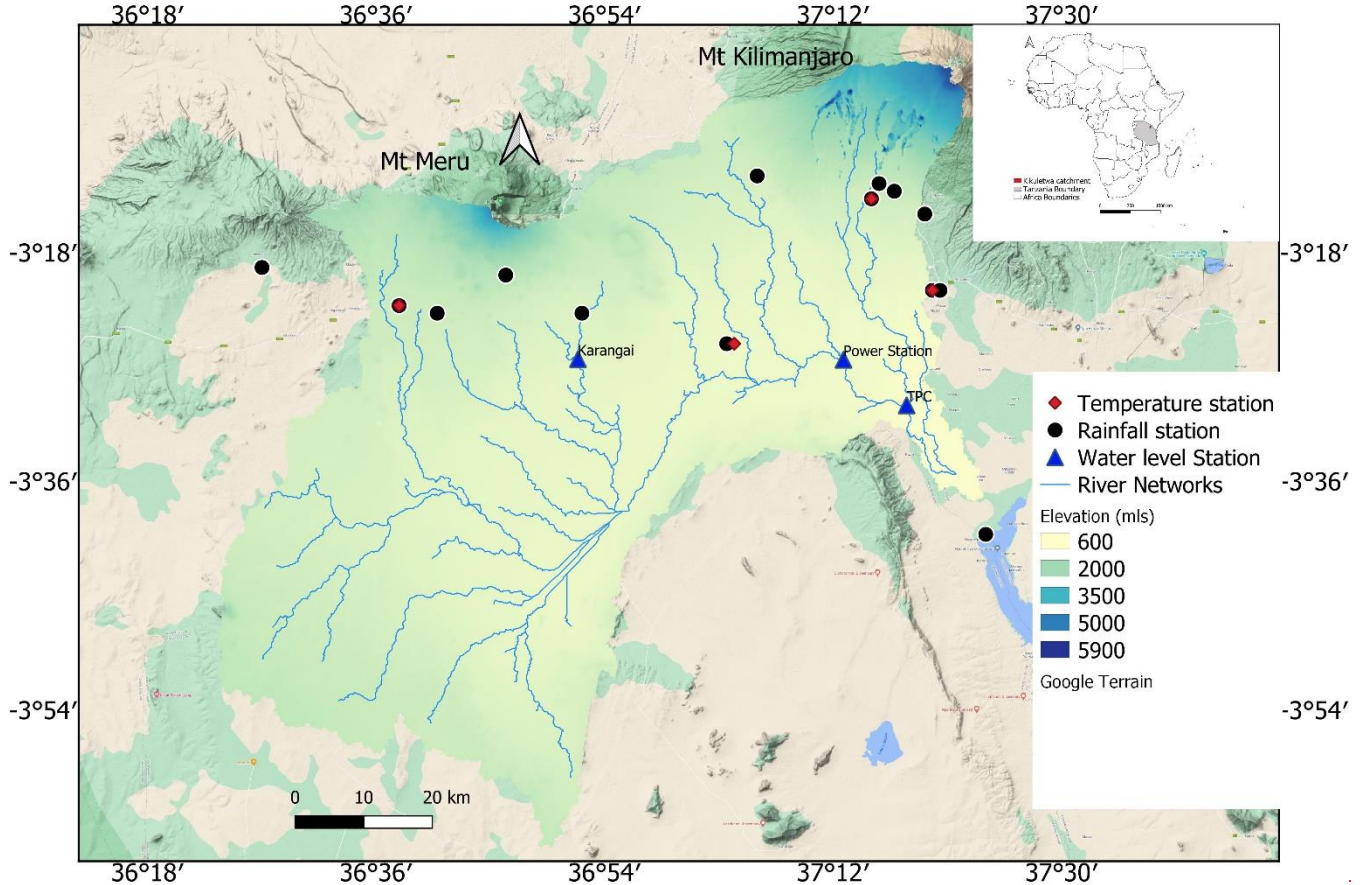
## 2. Methods

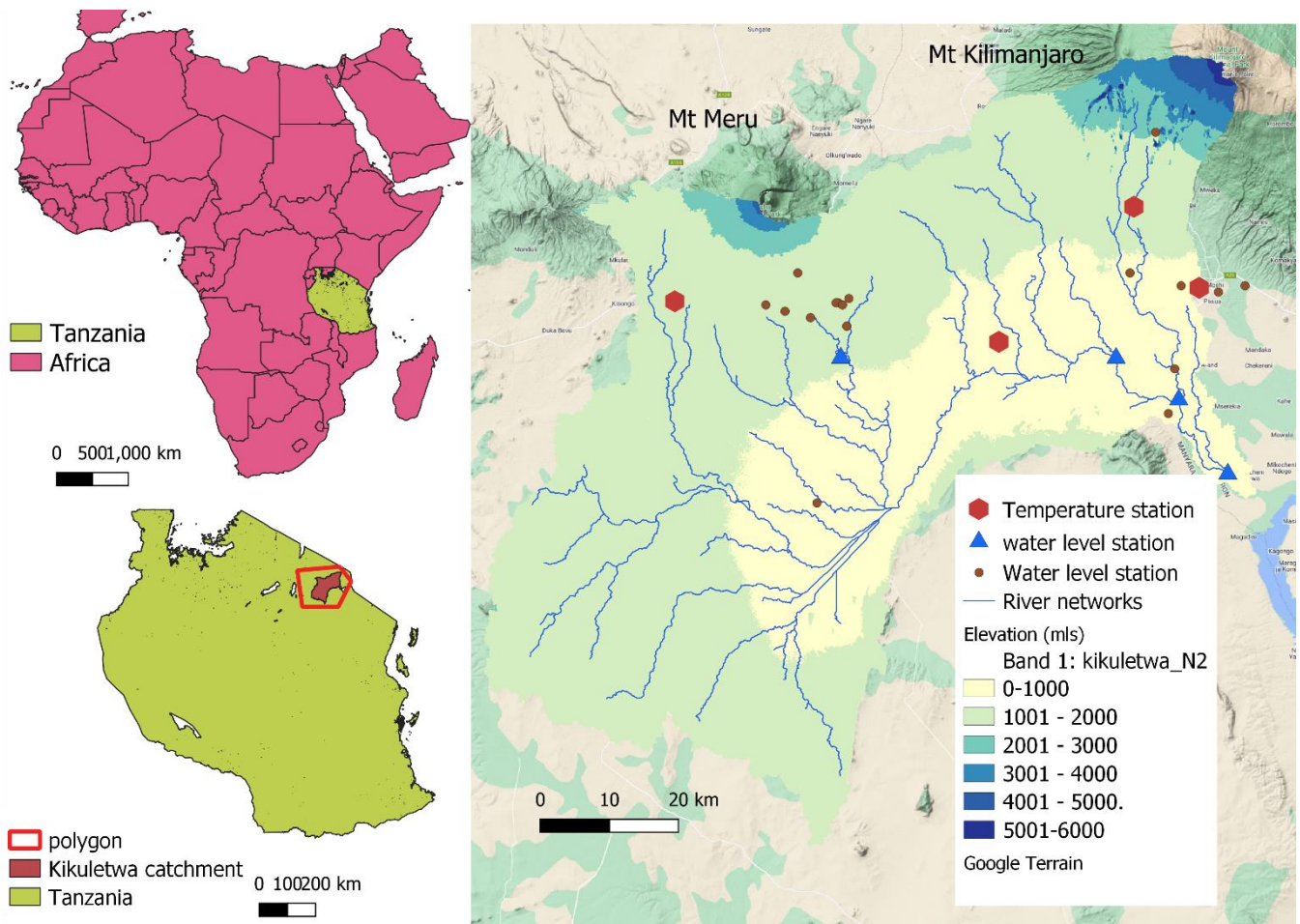
### 2.1. Study Area

The Kikuletwa basin is a sub-basin of the Pangani basin that covers approximately 6,650 km<sup>2</sup> (Figure 1).

175 Rainfall within the basin is bi-modalbimodal, meaning that the area receives long rains (masikaMasika) from March to June and short rains (vuliVuli) from November to December, as shown in Figure 2. Annual rainfall ranges between 300-800 mm in the lower part of the basin to 1200-2000 mm in the highlands of Mount Meru and Kilimanjaro. The maximum temperature ranges from 25 to 33<sup>0</sup>C and minimum temperature ranges from 15 to 20<sup>0</sup>C. The basin comprises of diverse LULC classes such as agricultural 180 land, dense forest on Mount Kilimanjaro (5880m) and Meru (4562m), grazed land, mixed urban and shrubland/thickets. Shrubland and thickets in the study area are found mainly in the lowlands where rain-fed agriculture is dominant. Urban areas concentrate around Arusha, although there are also emerging small towns. Moreover, grazed land is mainly found in the Maasai land of Monduli and Simanjiro districts. Irrigated agriculture in Kikuletwa is mainly practiced in the highlands and lowlands along the 185 river of Moshi, Moshi urban, Hai, Arumeru, Arusha, and Siha districts. The main crops in the highlands are banana, coffee, and maize, while the lowlands are dominated by mixed vegetable crops such as tomatoes, onions, and beans.



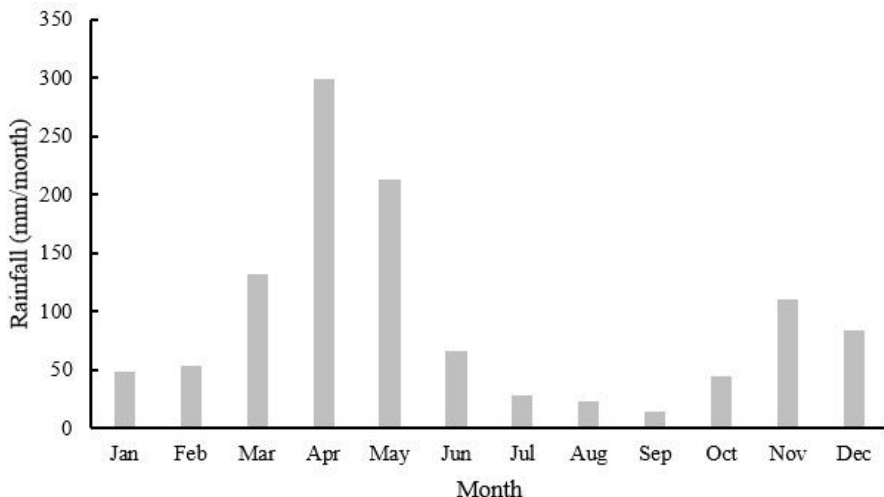




190

**Figure 1.** [Location and main features of the Kikuletwa basin with Google Terrain background in Tanzania](#)—The location of the Kikuletwa catchment in Africa (inset map). The catchment map shows the river networks and the location of ground water level, rainfall and temperature station in and around the catchment. (by Authors).

Average Monthly rainfall (2010-2016)



Average Monthly rainfall (2006-2016)

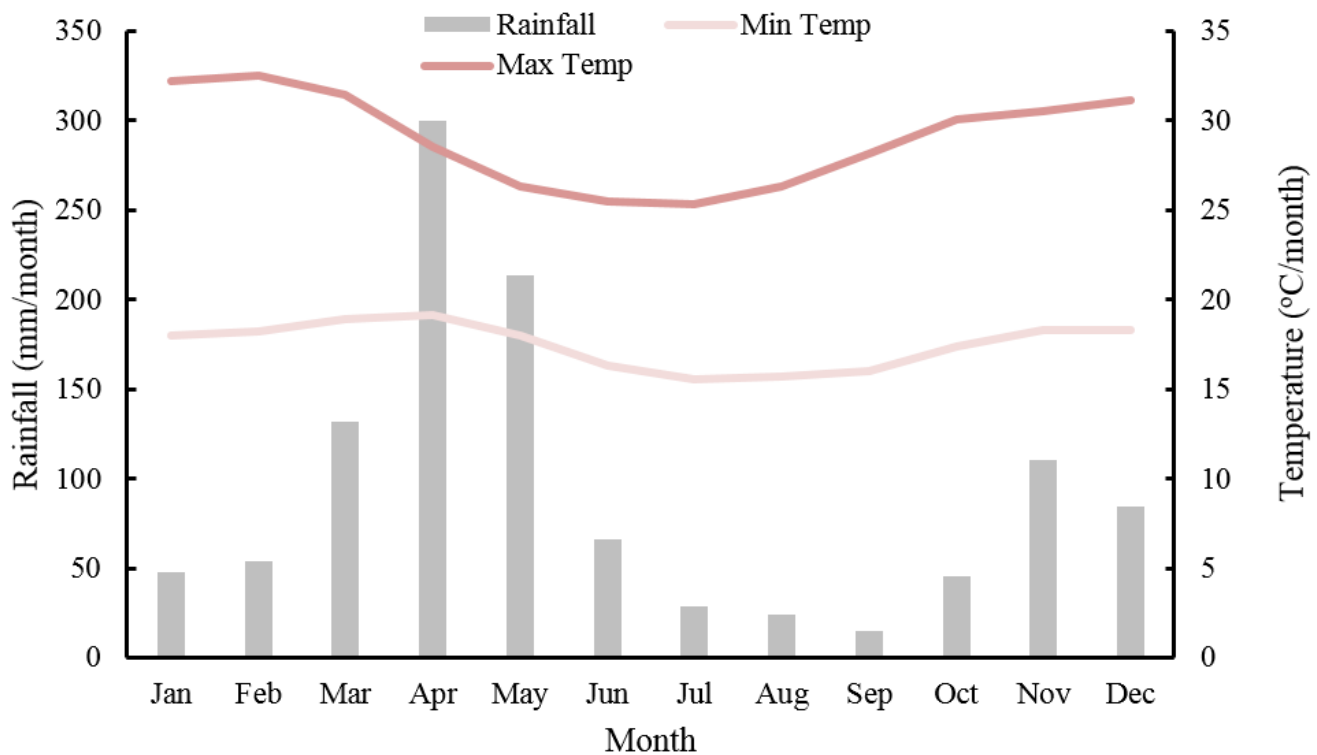


**Figure 2.** Monthly average rainfall (mm) [and temperature](#) of Kikuletwa basin ground rainfall stations

## 2.2 Input dataset for SWAT+

The required rainfall, river discharge, climate data, topography, soil map and land-use map were collected from different sources. The 90-m Shuttle Radar Topographic Mission (SRTM) 90m resolution Digital Elevation Model (DEM) was obtained from the United States Geological Survey (USGS) website (<https://earthexplorer.usgs.gov/>); the soil map was extracted from the African Soil Information Service (AFSIS; [Hengl et al., 2015](#)). Daily rainfall records for 10 stations were obtained from the Tanzania Meteorological Agency (TMA) and Pangani Basin Water Office (PBWO). Daily discharge records were obtained from PBWO. The daily climate records of temperature (maximum and minimum) for three stations were obtained from PBWO and TMA. The different data sets had variable record length and quality. However, for the selected 10 rainfall and 4 temperature stations, only good quality data records for the overlapping period (2006 to 2013) were selected.

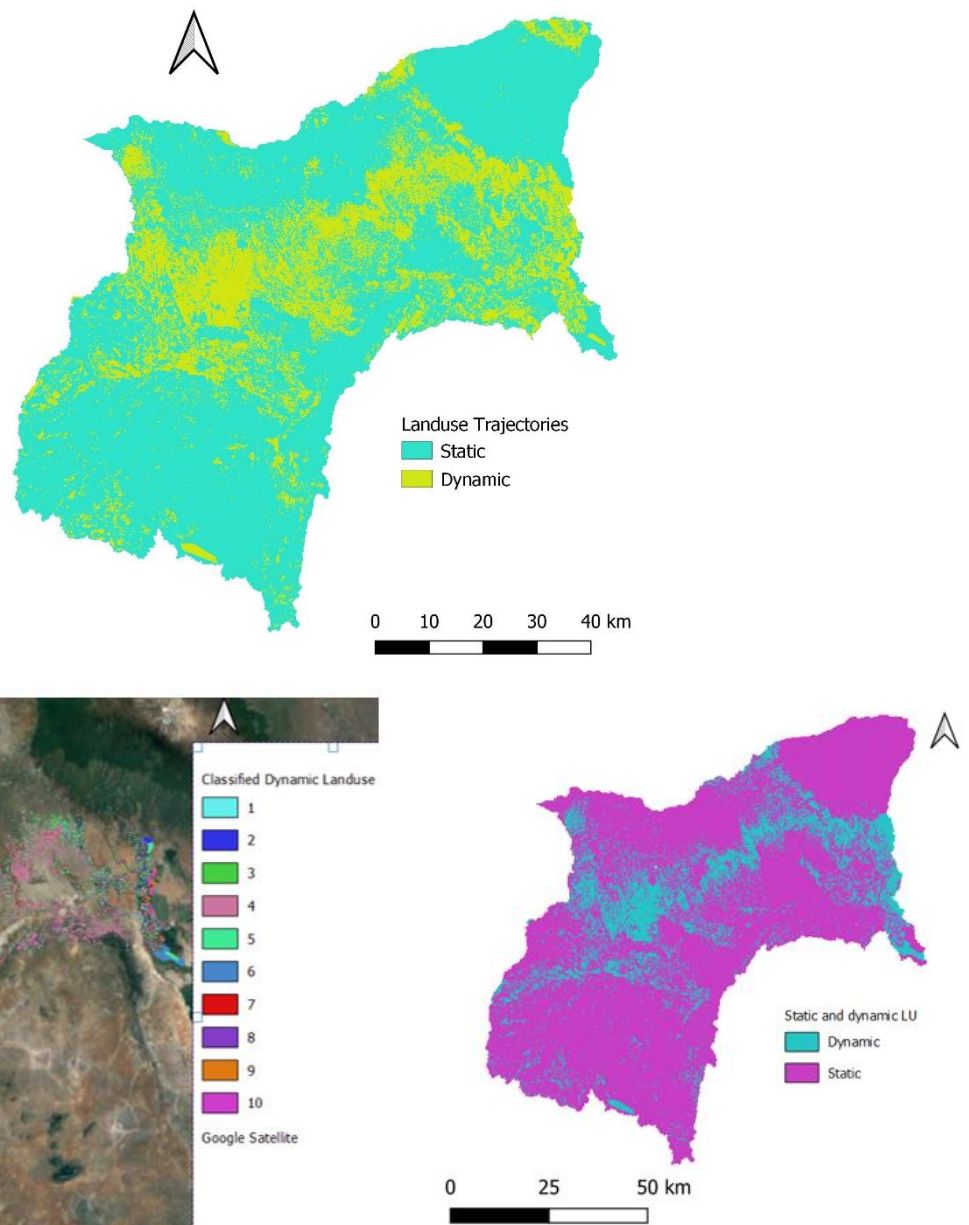
Our study used an improved LULC maps with local observation unlike other studies in the same catchment such as (Notter et al., 2012; Ndomba et al., 2008). For instance, Notter et al. 2012 used only a few herbaceous crops in model parametrization without a cropping calendar. The LULC maps were created using Landsat 8 (30m resolution) image of three months (March, August and October) representing three seasons in the basin ([Msigwa et al., 2019](#)). The March map represents the LULC during the long-wet season (*Masika*), the August map represents the dry season, and the October map represents the short rainy seasons (*Vuli*). The overall classification accuracy for the land use maps of March, August, and October 2016 were 85.5%, 88.5%, and 91.6% with a kappa coefficient of 0.84, 0.87 and 0.91, respectively ([Msigwa et al., 2019](#)). About 20 and 19 LULC classes in the Kikuletwa catchment were mapped for the wet and dry seasons, respectively. More details on the land use classes and their accuracies are found in Msigwa et al. (2019). The LULC maps were reclassified to match the SWAT land-use classification ([see Table 3B in Appendix B](#)). For instance, the SWAT land-use code 'PAST' was used to represent grazed grassland in the maps [see Table 3B in Appendix B](#).

## 2.3 Land-use Trajectories

The LULC change trajectory methodology has been widely applied in many areas to assess LULC change and its impact on the environment. Researchers use trajectories to analyse the change happening between 225 two images pixel by pixel (Mertens and Lambin, 2000; Swetnam, 2007; Zhou et al., 2008; Wang et al., 2012; Zomlot et al., 2017).

In this study, we extended the meaning of land-use trajectories from 'land-use change' to 'seasonal 230 succession of land-use types for a given sample unit (pixel) with more than two observations at different times' (Zhou et al., 2008). We applied the method in this study to assess the agricultural seasonal dynamics for the meteorological dry and wet seasons of the Kikuletwa basin.

The land-use change trajectories were obtained by integrating three classified images to represent the 235 three cropping seasons so that pixel-based change trajectories could be found using GIS. A land-use trajectory is the trajectory of a certain pixel in each of the three images. For example, a trajectory of 2→3→0 means for that pixel the land-use in March was rain-fed Maize (2), then in August, irrigated mixed crop (3) and finally, in October, Bare land (0). This type of trajectory is classified as dynamic, whereas a trajectory of 4→4→4 meaning the land-use is irrigated banana and coffee (4) in March, August, and October, is a static trajectory. Thus, the LULC change trajectories were categorized into dynamic and 240 static land-use trajectories. We only implemented the trajectories from all agricultural land-uses except irrigated banana and coffee and irrigated banana, maize and coffee land-uses which were combined as irrigated banana and coffee land-use. About 74% of the trajectories were static while 26% of the 245 trajectories were dynamic. Figure 3 shows the spatial distribution of static and dynamic land-use trajectories found in the study area. Only agricultural land-use and extensive agriculture LULC such as grazed grassland and shrubland were considered when analysing the seasonal changes (dynamic land-uses) and implemented in the SWAT+ model. We analyzed and implemented 40 land-use trajectories. Appendix B, Table 1B shows few trajectories that were implemented.



250 **Figure 3.** Spatial distribution of main dynamic and static land-use trajectories and distinction  
between dynamic and static land-use identified in the study area.

<u>Legend</u>		<u>Main Trajectory</u>	<u>Crop/ vegetation cover meaning</u>
<u>Id</u>			
1	<a href="#">AGRL-BSVG-AGRL</a>		Beans-space vegetation-beans
2	<a href="#">CORN-AGRL-PAST</a>		Rainfed maize-beans-grassland
3	<a href="#">CORN-AGRL-BSVG</a>		Rainfed maize-beans-space vegetation
4	<a href="#">AGRL-AGRL-BSVG</a>		Irrigated mixed crops- irrigated mixed crops -space vegetation
5	<a href="#">CORN-AGRL-AGRL</a>		Rainfed maize- Irrigated mixed crops - Irrigated mixed crops
6	<a href="#">AGRL-AGRL-AGRL</a>		Irrigated mixed crops - Irrigated mixed crops - Irrigated mixed crops
7	<a href="#">AGRL-AGRL-PAST</a>		Irrigated mixed crops - Irrigated mixed crops -grassland
8	<a href="#">AGRL-AGRL-PAST</a>		Irrigated mixed crops - Irrigated mixed crops -grassland
9	<a href="#">SUGC-AGRL-AGRL</a>		Irrigation sugarcane- Irrigated mixed crops - Irrigated mixed crops
10	<a href="#">AGRL-AGRL-AGRL</a>		Irrigated mixed crops - Irrigated mixed crops - Irrigated mixed crops

255

## 2.4. SWAT+ Model

SWAT+ is a physically based, semi-distributed hydrological model and a restructured version of the Soil and Water Assessment Tool (SWAT) designed to face present and future challenges in water resources modelling and management (Bieger et al., 2017). SWAT+ is more flexible in simulating the basin

260 processes such as evapotranspiration, runoff, crop growth, ~~nutrient~~nutrient, and sediment transport due to its watershed discretization and configuration. The HRUs are defined as a contiguous area, i.e., a representative field, with an associated user-defined length and width. The actual HRU is calculated based on the DEM, soil and land-use map inputs. Sub basins are delineated during the model construction, but they are divided into water areas and one or more landscape units (LSU) [\(Bieger et al., 2017\)](#) (Bieger et 265 al., 2017).

Land-use and management representation in SWAT+ can be done through the management file or using decision tables. Decision tables are an accurate yet compact way to model complex rule sets and their corresponding actions [\(Arnold et al., 2018\)](#). Nkwasa et al., (2020) highlighted the greater flexibility provided by decision tables during the representation of agricultural practices in SWAT+. The model

270 gives room for two or more crops growing at the same time by defining the plant community in the specific plant file. The model enables the representation of the reality of cultivated tropical basins.

The ET in the model is estimated at HRU level. There are different methods (Priestley-Taylor, Penman-Monteith and Hargreaves) used to estimate ET in the SWAT+ model. More detailed information can be found in (Abiodun et al., 2017; Neitsch et al., 2002; Alemayehu et al., 2016). Our study adopted the 275 Hargreaves method (Hargreaves and Samani, 1982) to estimate ET due to the limited amount of input dataset such as solar radiation. The method has been tested ~~to be useful~~ in tropical basins such as the Mara basin linking Tanzania and Kenya, ~~rather than using remote sensing climate data which is associated with uncertainties~~ (Alemayehu et al., 2016). ~~Our aim was to use available ground data and not rely on remote sensing climate data such as solar radiation which is reported to have -uncertainties~~ (Alemayehu et al., 280 2016). ~~SWAT model have also been successfully used in Pangani basin for different purposes~~ (Ndomba et al., 2008; Notter et al., 2012).

## 2.5 Land-use Trajectories Implementation in SWAT+

We combined ~~three~~ ~~land-use~~ maps (March, August and October) to obtain the trajectory land-use map. Forty land-use trajectories were produced from the three seasonal land-use maps. ~~These trajectories differ from the traditional approach as they not only use the agricultural statics but use land use maps to define the space.~~ Then each trajectory was assigned a ~~placeholder~~ SWAT+ land-use code ~~(placeholder)~~. For instance, a placeholder SWAT+ land-use code ~~'MIXC'~~ signifies ~~a trajectory~~ CORN → ~~AGRL TOMA~~ → ~~AGRL TOMA~~ trajectory (rainfed maize to tomato to tomato land use trajectory) or ~~'MIGS'~~ signifies ~~a~~ CORN → ~~AGRL TOMA~~ → BSVG trajectory (~~rainfed(rainfed maize to tomato to sparse vegetation land use trajectory)~~) as shown in ~~Table 1B of (a) Appendix B~~. ~~Further, the SWAT+ dynamic model was set up with the A trajectory land-use map represented with the placeholder SWAT+ land-use codes using the lookup Table 1B (Appendix B) for Kikuletwa basin was created.~~

~~The final model was then implemented by assigning each placeholder SWAT+ land-use codes according to its respective trajectory using the lookup Table 1B, in Appendix B.~~ A python code (Appendix A) was 295 used to ~~first~~ assign trajectories of the placeholder SWAT+ land-use codes, and to create the trajectories'

management files i.e.i.e., such as ‘landuse.lum’, ‘management.sch’ and ‘hru-data.hru’ files. In the ‘Landuse.lum’ file, the trajectories were defined with respect to the plant community. ‘Management.sch’ file controls the timing of the planting and harvesting of the individual crops in the community (Table 1). For instance, the tomato and soya beans are planted in the same field with different planting and harvesting schedules but grown at the same period. However, each crop was defined by its own plant community in new SWAT+ to make distinction between these crops. The ‘hru-data.hru’ file links the HRUs to the corresponding land-use management. The irrigation schedules were implemented using decisions tables. The sources of irrigation water in the catchment was river and irrigation techniques were mostly furrow. The irrigation schedules were implemented using decisions tables.

305 **Table 1.** An example of a ‘management.sch’ file input in dynamic SWAT+ model

<b>name</b>	<b>numb_ops<sup>9</sup></b>	<b>numb_auto<sup>10</sup></b>	<b>op_typ<sup>11</sup></b>	<b>Mon<sup>12</sup></b>	<b>Day<sup>13</sup></b>	<b>hu_sch<sup>14</sup></b>	<b>op_data1*</b>	<b>op_data2*</b>	<b>op_data3*</b>
cor_agr_agr_m <sup>1</sup>	8	2							
			irr_toma_soy <sup>2</sup>						
			irr_corn <sup>2</sup>						
			plnt <sup>3</sup>	3	15	0	corn <sup>5</sup>	grain <sup>8</sup>	0
			hvkl <sup>4</sup>	8	15	0	corn	grain	1
			plnt	7	1	0	soyb <sup>6</sup>	grain	2
agr_agr_agr_m <sup>1</sup>	8	2							
			plnt	8	20	0	toma	null	3
			hvkl	10	1	0	soyb	grain	4
			hvkl	10	20	0	toma <sup>7</sup>	null	5
			plnt	10	30	0	corn	grain	6
			hvkl	2	28	0	corn	grain	7
			irr_toma_soy <sup>2</sup>						
			irr_corn <sup>2</sup>						
			plnt	3	15	0	soyb	grain	0
			hvkl	6	30	0	soyb	grain	1
			plnt	7	1	0	soyb	grain	2
			plnt	8	20	0	toma	null	3
			hvkl	10	1	0	soyb	grain	4
			hvkl	10	20	0	toma	null	5
			plnt	10	30	0	corn	grain	6
			hvkl	2	28	0	corn	grain	7

<sup>1</sup> name of the land-use management, <sup>2</sup> points to the irrigation decision tables, <sup>3</sup> planting operation, <sup>4</sup> harvesting operation, <sup>5</sup> rainfed maize, <sup>6</sup> soy bean, <sup>7</sup> tomato, <sup>8</sup> harvest the grain portion of the crop, <sup>9</sup> number

of operations, <sup>10</sup> number of auto-operations, <sup>11</sup> operation type, <sup>12</sup> month, <sup>13</sup> day, <sup>14</sup> heat unit schedule, \*

310 operations

## 2.6 Model Configuration for both Static and Dynamic SWAT+ Models

The SWAT+ model was setup using DEM, soil map and land-use map of March 2016 for the static representation scenario ([sStatic model](#)) and using a trajectory map [and files \(described in section 2.5\)](#) for the dynamic representation scenario ([dynamic Model](#)). [In the static model the crops were grown in the rain seasons from March till July and the land would be left bare. This is normally the case with most SWAT model Application in SWAT](#) (Ndomba et al., 2008; Gashaw et al., 2018; Koch et al., 2012).

315 [The same](#) ground observations of rainfall and temperature were used (Appendix C, Table 1C) [for both models](#). The precipitation stations were adjusted manually according to elevation and the potential maximum leaf

area [index of maize](#) was adjusted to correspond to the field measurements of the basin. USDA Soil

320 Conservation Service (SCS) curve number was used to estimate surface runoff [and first order markov chain for rainfall distribution](#) and [the muskingum method used for](#) channel routing.

For the static SWAT+ model, 23 sub-basins, 171 land scape units and 6086hru were generated with 14 land-use classes, while for the dynamic SWAT+ model, 23 sub-basins, 171 land scape units and 9333hru were generated with 40 land use classes representing the 40 different trajectories. The difference in the

325 number of HRUs is related to the higher number of land-use classes in the dynamic land-use mapping.

[The irrigation schedules were implemented through decisions tables \(Arnold et al., 2018\) by specifying a furrow irrigation method and using the rivers within the sub-basins as the source of irrigation. The model was run from for a period of 8 years \(20068 to 2013\). The year 2006 and 2007 first two years were used as a warm up period. was a warming period.](#)

## 330 2.7 Model Evaluation

Both the static and dynamic SWAT+ models were compared on how they simulate the water balance [and with specific focus on the ET component since evapotranspiration estimations as the focus of this study is aims at mainly to improve improving the spatial distribution of blue and green water consumption. and](#)

~~not discharge simulation, is to estimate the land use fluxes to estimate blue and green water consumption.~~

335 ~~Hence, the SWAT+ models was were not calibrated.~~ The ET from both static and dynamic SWAT+ representation scenarios ~~at basin level were was~~ compared with the remote sensing ET ~~at a basin level for the same simulation period from 2008 to 2013~~. The remote sensing ET is an ensemble ET product from ~~six seven~~ existing global scale ET products [\(IHE Delft, 2020\)](#) (IHE Delft, 2020). [All the ET products are based on multi-spectral satellite measurements and surface energy balance models i.e.: Global Land](#)

340 [Evaporation Amsterdam Model \(GLEAM\)](#) (Miralles et al., 2011), [CSIRO MODIS Reflectance-based Evapotranspiration \(CMRS-ET\)](#) (Guerschman et al., 2009), [Operational Simplified Surface Energy Balance \(SSEBop\)](#) (Senay et al., 2013), [Atmosphere-Land Exchange Inverse Model \(ALEXI\)](#) (Anderson et al., 2007), [Surface Energy Balance System \(SEBS\)](#) (Su, 2002), [ETMonitor](#) (Hu and Lia, 2015) [and MODIS Global Terrestrial Evapotranspiration Algorithm \(MOD16\)](#) (Mu et al., 2011). [The ET maps produced by IHE Delft have a resolution of 250x250m at a monthly scale. The detailed information on the ET products description and method are found in \(Hugo et al., 2019\).](#) The product was evaluated for the study area by comparing the basin water balance at three gauged stations; Karangai, Kikuletwa Power station and Tanzania Plantation Company (TPC) over a period of six years (2008-2013). The comparison of ET calculated using the water balance and remote sensing showed good agreement (NSE= 0.77) for

345 [Kikuletwa Power station which covered 86% of the total basin area \(Msigwa et al., 2019, 2021\)](#) ([Msigwa et al., 2019](#)). Statistical metrics such as Nash-Sutcliffe efficiency (NSE), Root Mean Square Error (RMSE), Percent Bias (PBIAS) and adjusted R squared ( $R^2$ ) were used to evaluate the both monthly ET from static and dynamic SWAT+ [models](#) against the remote sensing ET. [Moreover, the Paired T-test statistical analysis was performed to find if there is significant difference between the ET from the static model and that of dynamic model for only the dynamic land uses.](#) [NSE is a normalized statistic that determines the relative magnitude of the residual variance \("noise"\) compared to the measured data variance \("information"\) \(Nash and Sutcliffe, 1970\).](#) [NSE is computed as shown in Eq. \(1\):](#)

$$NSE = 1 - \left[ \frac{\sum_{t=1}^n (Y_t^{obs} - Y_t^{sim})^2}{\sum_{t=1}^n (Y_t^{obs} - Y_t^{mean})^2} \right] \quad (1)$$

RMSE is one of the commonly used error index statistics in many models (Kiptala et al., 2014; Jia et al.,

360 Yang et al., 2016; Miralles et al., 2011). RMSE is computed as shown in Eq. (2):

$$RMSE = \left[ \sqrt{\sum_{i=1}^n (Y_i^{obs} - Y_i^{sim})^2} \right] \quad (2)$$

PBIAS measures the average tendency of the simulated data to be larger or smaller than their observed data (Gupta et al., 1999). The ideal value of PBIAS is 0.0, with low magnitude values indicating accurate model simulation. Positive values indicate model underestimation bias, and negative values indicate model overestimation bias (Gupta et al., 1999). PBIAS is calculated with Eq. (3):

$$PBIAS = \left[ \frac{\sum_{i=1}^n (Y_i^{obs} - Y_i^{sim})}{\sum_{i=1}^n (Y_i^{obs})} * 100 \right] \quad (3)$$

R<sup>2</sup> describes the degree of collinearity between simulated and measured data. It describes the proportion of the variance in measured data explained by the model. R<sup>2</sup> ranges from 0 to 1, with higher values indicating less error variance, and typically values greater than 0.5 are considered acceptable (Santhi et al., 2001). For more details of statistical matrices, see Moriasi et al., (2007).

## 2.8 Estimating blue and green ET

The blue ET is a portion of crop evapotranspiration after application of irrigation while green ET is the evapotranspiration as a result of rainfall. The blue ET in this study was estimated as a difference between

375 ET under irrigation and ET without irrigation (Liu and Yang, 2010). The SWAT+ dynamic land-use implementation was run without irrigation and then later irrigation was applied. The green ET is the actual evapotranspiration from precipitation which can be kept in unsaturated soil and absorbed by plants and is then returned to the atmosphere via evapotranspiration. In this study, only the portion of blue water consumed from irrigation was considered and not all the blue water resources like other studies (Xie et al., 2020).

380

The SWAT+ model was run first assuming that no irrigation was carried out. The computed ET is called  $ET_{green}$ . Then the SWAT+ model was run again with irrigation being implemented and the ET computed is called  $ET_{total}$  as explained in the two scenarios below.  $ET_{blue}$  is computed by the difference of  $ET_{total}$  from the run with irrigation implantation and  $ET_{green}$  “Eq. (4)”.

385 The two scenarios to estimate blue ET

1. The seasonal dynamic SWAT+ is carried out by assuming the soil does not receive any irrigation water. The evapotranspiration computed using this first run is referred to as  $ET_{green}$
2. The seasonal dynamic SWAT+ is carried out by assuming the soil receives sufficient irrigation water. The evapotranspiration computed using this second run is referred to as  $ET_{total}$

390 Hence,  $ET_{blue}$  is computed from the “Eq. (4)” below

$$ET_{blue} = ET_{total} - ET_{green} \quad (4)$$

It should be noted that the trajectory implementation involves only two of the agricultural land-uses i.e. rainfed maize and mixed crop with exception of irrigated banana and coffee land-use and irrigated banana, coffee and maize land-use.

395 **2.9 Comparison of SWAT+ results with other remote sensing methods**

The SWAT+ blue and green ET were ~~compared~~ compared with the results from the four remote sensing data based methods namely: SN (Senay et al., 2016), EK (van Eekelen et al., 2015), Budyko method (Simons et al., 2020) and Soil Water Balance method -SWB (FAO and IHE Delft, 2019).

400 The SN method (Senay et al., 2016) is the simplest method whereby blue water is estimated as a difference between precipitation (P) and ET, followed by the modified method of van Eekelen et al., (2015) where the effective fraction was introduced to reduce the amount of precipitation that evaporates. The Budyko method, as described in Simons et al., (2020), estimates green water from precipitation using an empirical relationship between actual evapotranspiration, precipitation and reference evapotranspiration. The Budyko equation, also called the Budyko curve, assumes a relationship between the evaporation ratio (ET/P) and climate aridity index (ET<sub>0</sub>/P) to describe the water-energy balance for long term analysis.

The soil moisture balance model computes green (ETgreen) and blue (ETblue) water components of ET, by keeping track of the soil moisture balance and determining whether ET can be satisfied through direct precipitation and precipitation stored as soil moisture alone or if an additional water (surface or groundwater supply) is required. The study compares blue and green water estimations for all LULC 410 classes for the Kikuletwa catchment. Further detailed description of each method is presented below.

### 3. Results

#### 3.1 Comparison of Simulated basin ET from Remote Sensing

Figure 4 shows the average monthly ET at the basin scale of Kikuletwa for the two model scenarios of SWAT+ and that from remote sensing. The dynamic SWAT+ model shows higher ET (by 20mm/month) 415 matching the remote sensing pattern in the dry seasons (July to October) than the static SWAT+ model implementation. This shows that there are agricultural activities occurring in the dry seasons. In the dynamic SWAT+ model, we implemented irrigation irrigated cropping during the dry seasons on the growing crops, which led to an increase in ET.

The statistical analysis (Table 2) shows that both the SWAT+ simulations have a correlation ( $R^2$ ) of above 420 0.5, when compared with monthly remote sensing monthly ET. However, the monthly average ET value for the dynamic land-use scenario is closer to the remote sensing ET, especially during the dry months from July to November where we implement more than one cropping season.

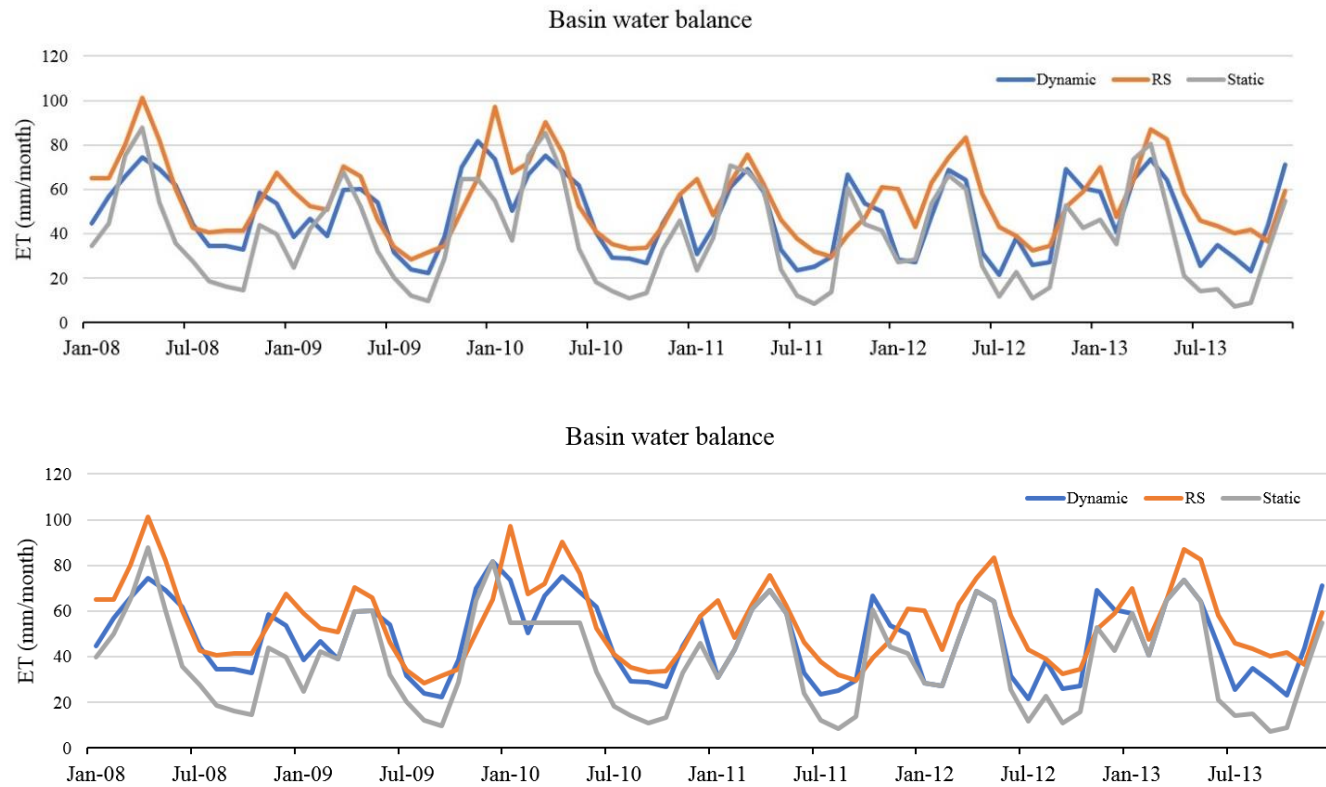
Unlike the commonly used static land-use scenario where only one cropping season was implemented per year, the monthly ET for the dynamic SWAT+ model implementation shows acceptable PBIAS of 13% 425 whereas, the static SWAT+ model shows higher PBIAS of 30%. Moreover, the dynamic SWAT+ model shows a good NSE of 0.4 while the static SWAT+ shows very low performance with an NSE of -0.46.

Table 3 shows the water balance component for the two scenarios. The A notable difference is seen in ET increase (24%) and decrease in other water balance components (lateral flow; 27%, percolation; 42%, surface runoff; 32%). The mass balance (change in soil water balance) in percentage for the static SWAT+ 430 model is higher (1.8%) than the dynamic SWAT+ model (0.5%). The most pronounced differences are

found when comparing the dynamic land-use representation on basin scale and the commonly used static land-use approach with remote sensing. Figure 5 shows the spatial distribution of ET from remote sensing, dynamic land-use and static land-use representation.

The average basin ET is 461mm/y, 573mm/y and 642 mm/y for the static SWAT+ model, dynamic 435 SWAT+ model, and remote sensing, respectively. Generally, all the simulated ET from SWAT+ shows lower annual average ET than remote sensing ET. However, the ET from static land-use representation shows a higher difference of 181mm/y whereas with the use of dynamic land-use, the difference in ET is only 69mm/y. [The paired T-test results show that there is a significant difference between the ET from the static model and that of the dynamic model for the dynamic land-uses. A P value of 0.013 was obtained, which was less than the 0.05 confidence interval.](#) Spatial distribution of ET from the SWAT+ models is different from remote sensing. However, visually, the spatial distribution of ET from the dynamic land-use scenario is closer and shows similar patches to remote sensing than the ET from the static land-use scenario (Figure 5).

The differences in ET spatial distribution (Figure 5) are vivid mostly in the trajectory implemented areas 445 in the lowlands see Figure 3. [Figure 6 shows the ET on the dynamic land-uses alone, the differences of the amount of the ET in these areas is more than 100mm per year. The vivid differences are seen on the right lower corner of the catchment where the differences in ET are more than 200mm/y. There are more areas with less than 400mm/y in the static model as compared to the dynamic model. However, the pattern of ET in SWAT+ is also influenced by the rainfall pattern. Likewise, the changes seen in the high land 450 areas of irrigated banana and coffee and the forested areas might be due to the increase in the number of HRUs in the dynamic SWAT+ model that contributed to the more accurate results.](#)



**Figure 4.** Average monthly ET for basin-scale summarized from remote sensing, dynamic land-use scenario and static land-use scenario.

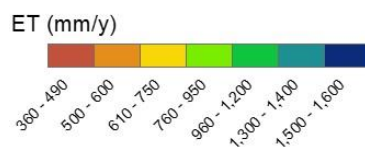
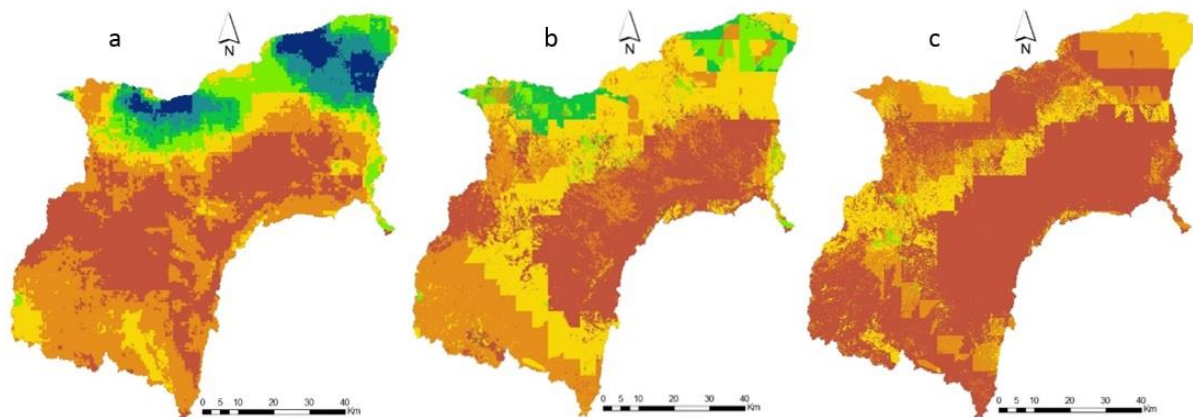
455

**Table 2.** Statistical analysis of ET comparison of SWAT scenarios from Remote sensing

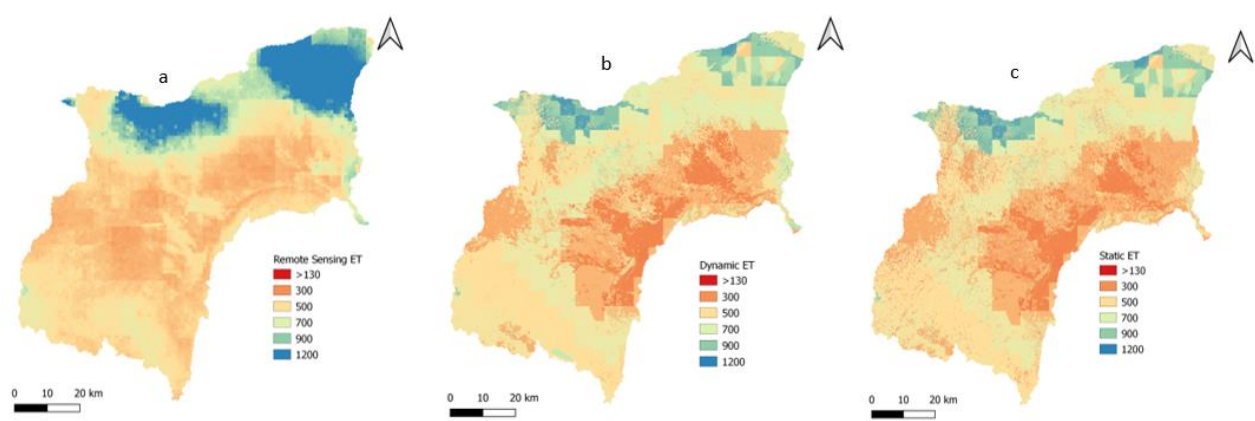
Statistic Parameter	Static SWAT+	Dynamic SWAT+
PBIAS	30%	13%
Nash-Sutcliffe efficiency (NSE)	-0.46	0.4
Adjusted R Square	0.6	0.6
RMSE (mm/month)	20.8	13.3

**Table 3.** Comparison of water balance component for the basin level

<b>Water balance component (mm)</b>	<b>Static</b>	<b>Dynamic</b>
Precipitation	814	814
Irrigation	0	8.25
Evapotranspiration	461	573
Lateral flow	139	101
Surface runoff	207	140
Percolation	21.7	12.6
%mass balance	1.8	0.53



460



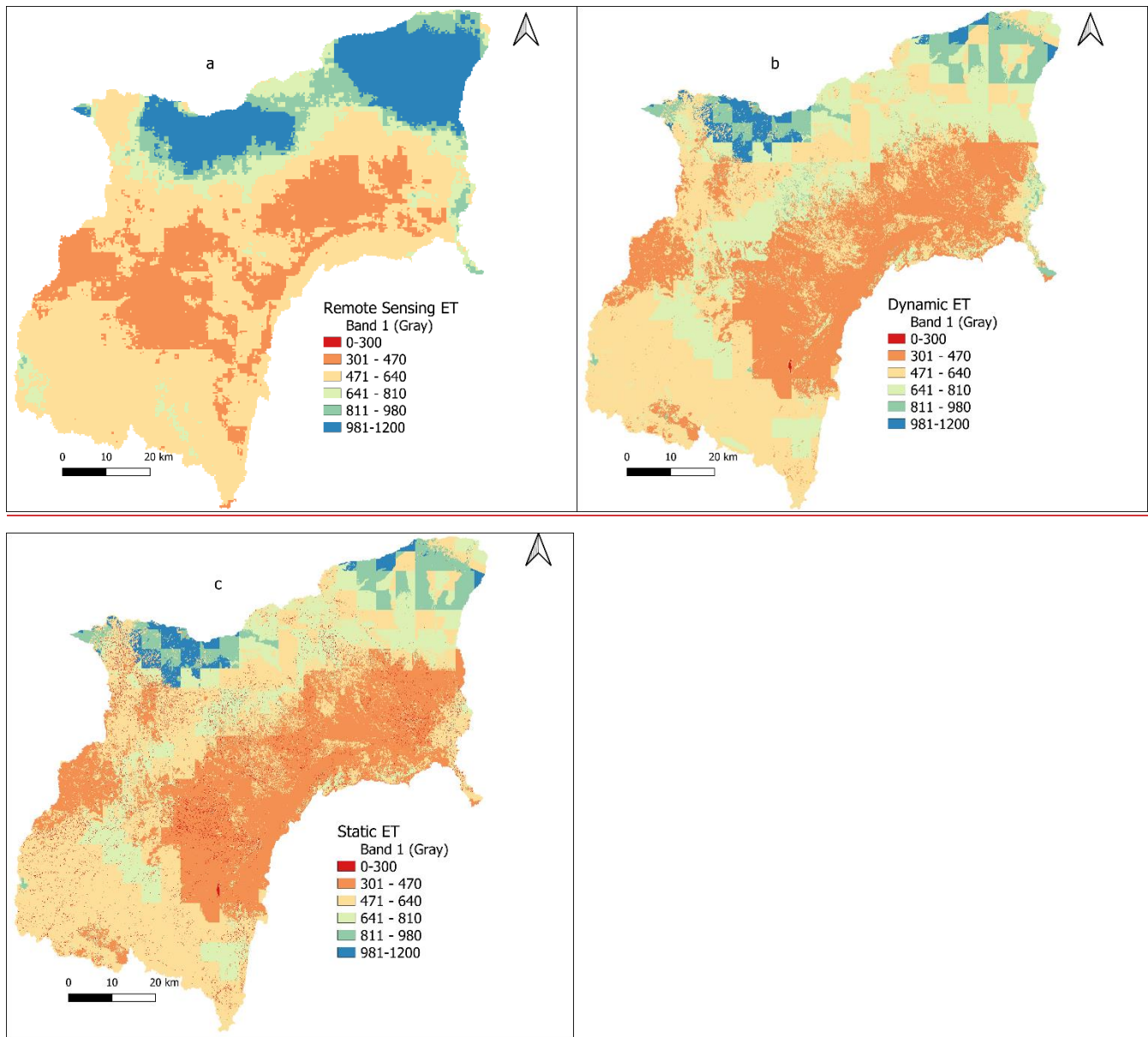


**Figure 5.** Spatial distribution of ET from a) Remote sensing b) dynamic land-use scenario and c) static

465 land-use scenario.

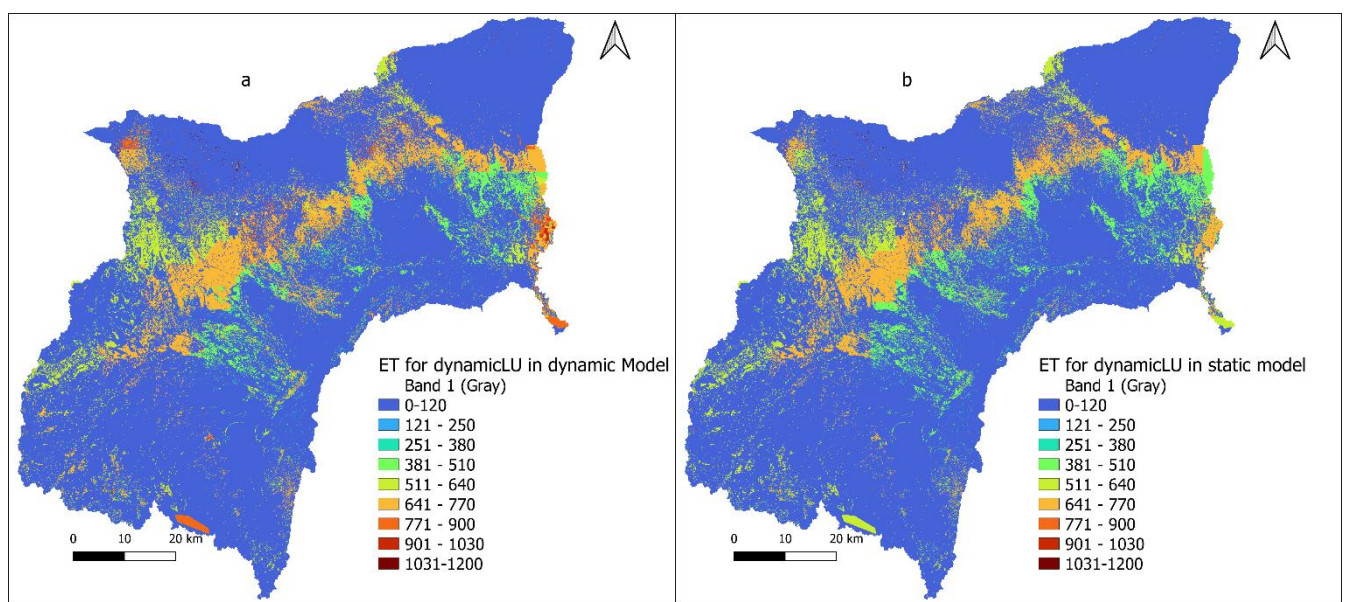
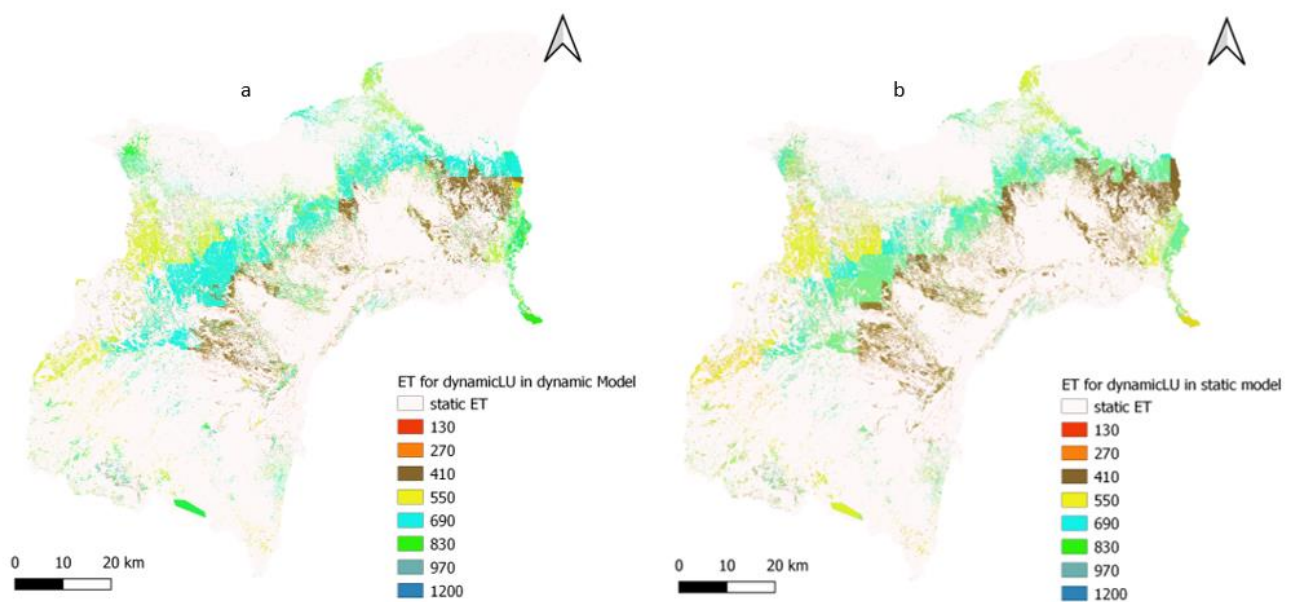


**Figure 6.** Spatial distribution of ET from dynamic Land-use for both a) dynamic and b) static SWAT+ Models.

Figure 6-7 shows the trends of blue and green annual ET in the Kikuletwa basin for annual (Figure 6) and from a period from 2008 to 2013. The implemented blue and green ET were mainly for irrigated mixed crop land-use due to implementation of trajectories. The annual average blue ET for irrigated mixed crops is 138mm which accounts for 25.5% of the annual average total ET and the annual average green ET is 475 402mm which accounts for 74.5% of the annual average total ET.

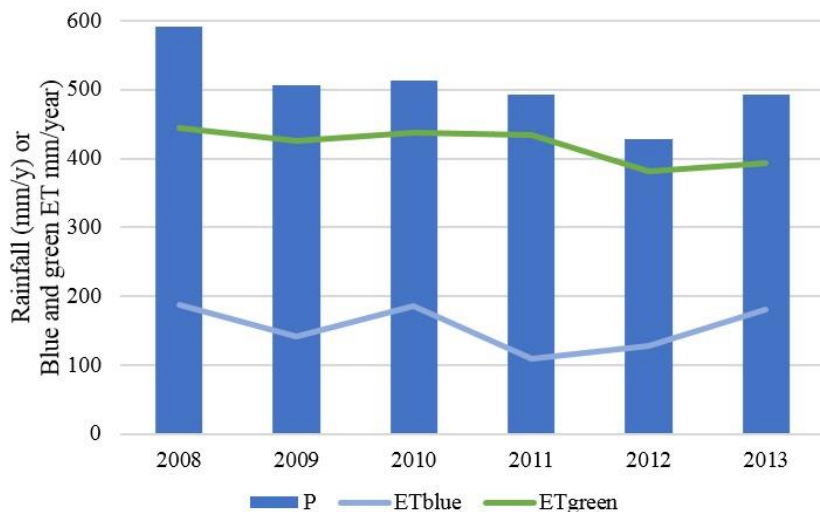
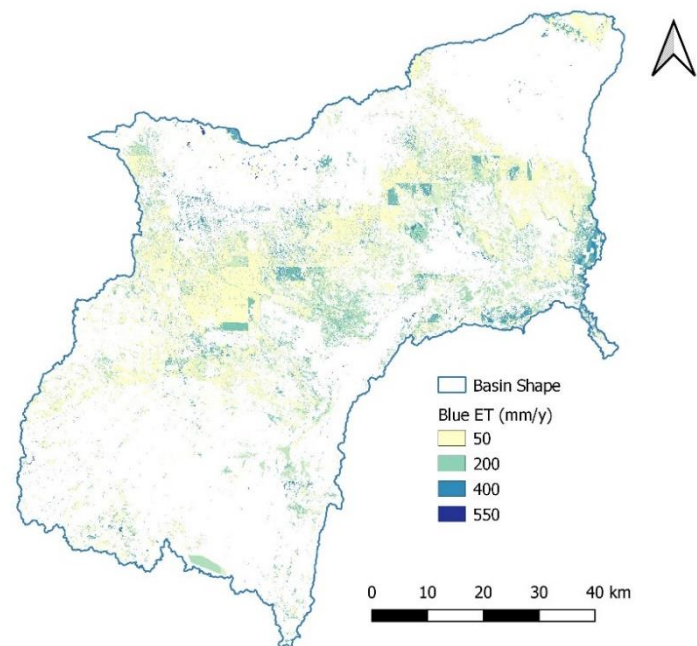
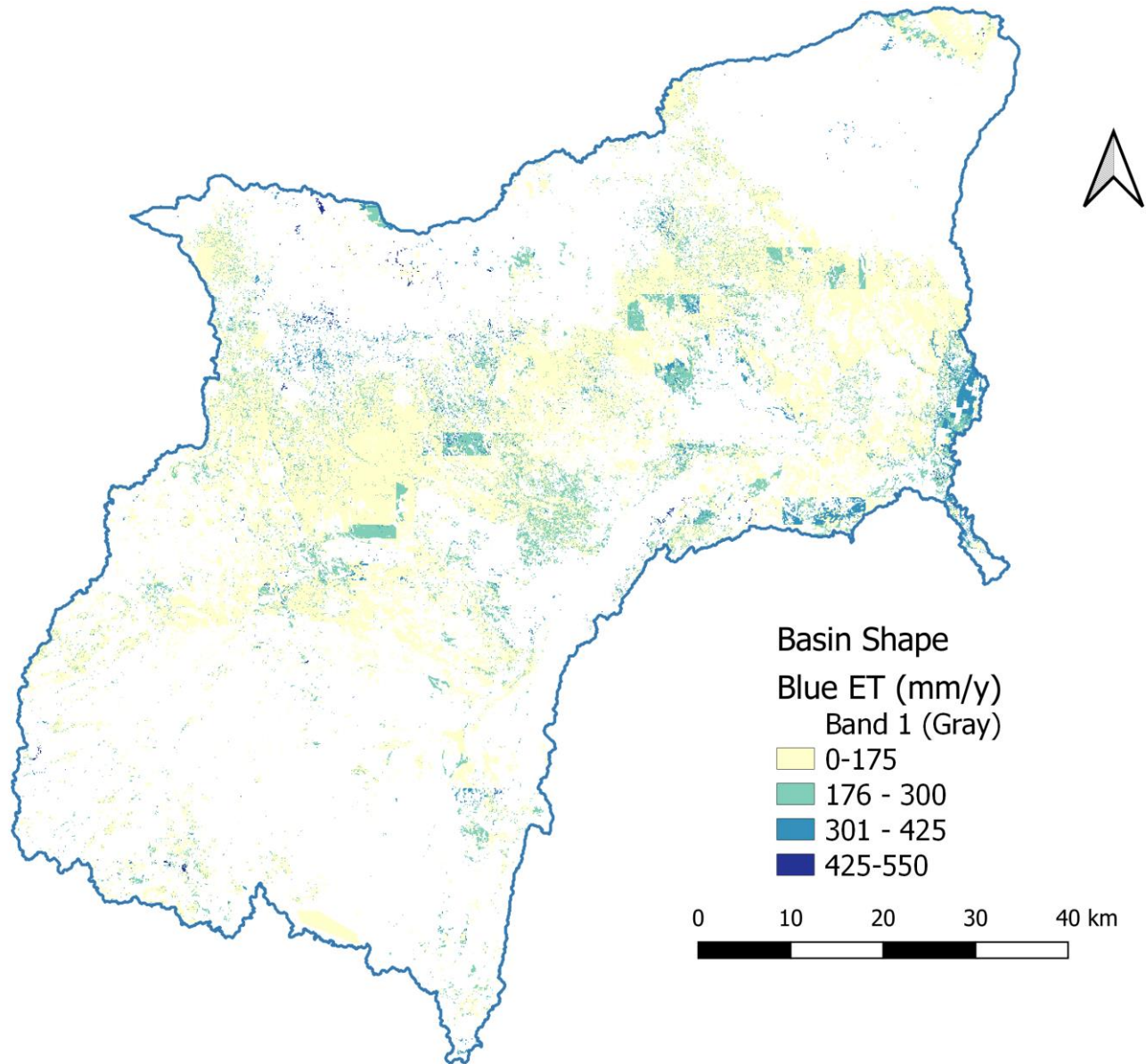


Figure 6-7. The annual variation of blue and green ET for from 2008–2013.

Figure 7-8 shows that the spatial distribution of blue ET for agricultural areas in the Kikuletwa basin for implemented trajectories such as rainfed maize to tomato to irrigated maize land use trajectory. (See 480 Appendix 2, Table 2). The blue water is calculated from the irrigated implemented trajectories that mainly include irrigated mixed crops (soybeans, tomato and irrigated maize). Figure 7-8 shows that more than half of the total area consumes less than 200mm of blue ET. The higher blue ET is seen in the lower right corner where the irrigated sugarcane plantation is found.





485

**Figure 78.** Spatial distribution of Blue ET for the implemented trajectories of rainfed and irrigated mixed crops land-use.

Figure 8-9 shows the comparison of average blue and green ET from four methods (Msigwa et al., 2021) (Msigwa et al 2021 *forthcoming*) with dynamic SWAT+. The value of both blue and green ET is closer to two methods, EK (van Eekelen) and SWB (Soil Water Balance) methods, which were indicated

490

to have realistic values of blue and green ET. Van Eekelen et al., (2015) is the method that analysed precipitation (P) and ET, and ET and applied an effective rainfall factor since not all rainfall will infiltrate and be stored in the unsaturated zone to be available for uptake by plants. Both ground data and remote sensing data could be used for data analysis-based approaches on an annual basis. The SWB model is a 495 pixel by pixel vertical soil water balance model that splits green and blue ET by tracking of soil moisture balance and determining if the ET is satisfied only from rainfall or stored in the soil moisture or additional sources if required (FAO and IHE Delft, 2019).

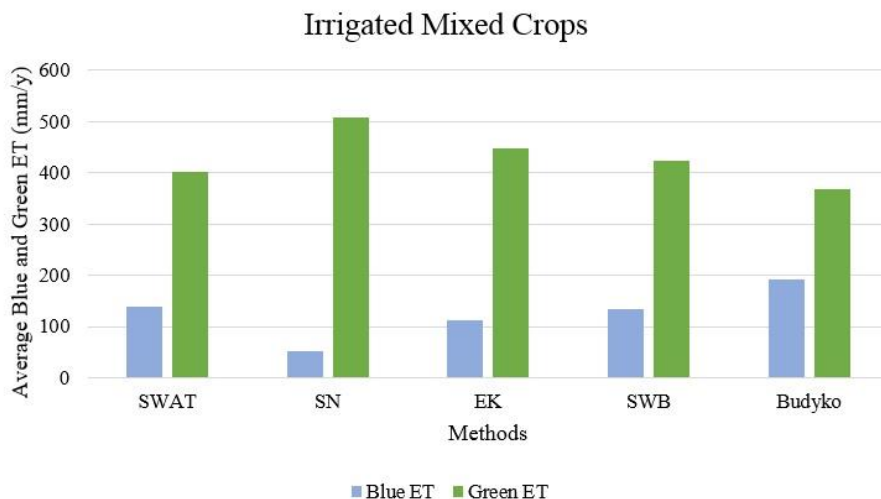


Figure 89. Blue and green ET comparison with other four methods from [forthcoming publication by Msigwa et al., \(2020\)](#) [Msigwa et al., \(2021\)](#).

#### 4. Discussion

Some previous studies have represented annual land-use changes in SWAT and found that these have a significant impact on hydrology (Wagner et al., 2016; Woldesenbet et al., 2017; Wagner et al., 2019) [\(Wagner et al., 2016, 2019; Woldesenbet et al., 2017\)](#). However, none of these studies has 505 represented the seasonal dynamics of land use within a single year [in a spatially distributed manner](#). Nkwasa et al., (2020) incorporated the seasonal land-use dynamic in SWAT and SWAT+ and found that models led to an improved vegetation simulation. This study did not show how the seasonal land-use

dynamic improved water balance component such as ET. Our study uses of agro-hydrological model (SWAT+) to represent blue and green ET for different cropping seasons (represented by trajectory with time and space) and the use of remote sensing ET to evaluate the simulated ET from SWAT+. The study 510 has compared a common default modelling approach where a static land-use map is used together with its management practices and a seasonal dynamic land-use representation where more than one ~~cropping~~ ~~cropping season~~ is represented in a year. The spatial and temporal ET estimates from two model setups were compared with remote sensing ET. An increase of 112mm/y of the ET is seen when seasonal 515 dynamic land-use is implemented in the dynamic model to match the remote sensing ET as compared to when a static land-use map is used in the static model. The ET results from the dynamic model are significantly different from the ET in the static model for the dynamic land-use. The models show differences in water balance components, this is due to implementation of the land-use trajectory in the dynamic model.

520 A remarkable difference is seen in the spatial distribution of ET from static and dynamic land-use SWAT+ representation. The dynamic land-use SWAT+ visually is similar to a remote sensing map compared to the static land-use SWAT+. This is because of the added management practices such as ~~irrigation~~ irrigated cropping in the dry seasons, unlike the default SWAT+ ~~where there were no activities in the dry~~ 525 ~~seasons~~ with a static land use throughout the simulation period. The ET from dynamic land-use setup could not reach maximum satellite ET because the satellite ET estimates also have uncertainties in the mountainous areas because of the presence of cloud cover. Moreover, different ~~data~~ methods for estimating ET could lead to these differences. Rainfall ~~Climate~~ ground stations (temperature, wind speed, relative humidity and solar radiation) were used for ET simulation in SWAT+ model while the remote sensing use the energy balance models, mostly remote sensing data.

530 On the other hand, the ET from the static land cover such as forest from the static and dynamic model setup show different ET values this could be because of the difference in the initial model setup. The model setup for static used a March land use map with only 14 land use classes, while the dynamic model used a land use map with 40 trajectories. Hence, the changes in the ET might be due to the different land

use maps yielding different number of HRUs. In order to avoid such difference, one could have a initial

535 setup with same land uses then trajectory implementation could only be with the agricultural land use

Furthermore, the ET estimates from the dynamic SWAT+ model were used to estimate blue and green ET. The blue and green ET estimates from SWAT+ for the mixed crop land-use show no significant difference in the values from the two methods (EK and SWB) assessed in the [\(Msigwa et al., 2021\)](#) [upcoming paper by Msigwa et al., \(2021\)](#).

540 These findings demonstrate the importance of the representation of seasonal land-use dynamic in modelling ~~hydrological models when quantifying~~ blue and green water consumption. Normally, most

models use NDVI to represent seasonal changes (Amri et al., 2011; Ferreira et al., 2003), whereas the use of dynamic land-use leads to improved accuracy of seasonal simulations of the water uses (Nkwasa et al., 2020). Seasonal land-use maps can add information on management practices of changes in temporal crop

545 rotation and irrigation water use at a spatial scale. However, to account for accurate seasonality of land-use, more than 3 maps within a year should be represented, ideally 12 maps each year. This would enable a more complete understanding of the agricultural land-use classes and minimize errors in the trajectory analysis. [However, Landsat 8 is associated with cloud most especially in the rainy season. Cloud masking techniques is needed before further analysis of the images. Also, there were uncertainties associated with](#)

550 [the trajectories for example unrealistic trajectories like change from crop to forest then crop again. These types of trajectories were corrected and reclassified.](#)

The Landsat 8 images used in this study to map seasonal land-use dynamics did not have a revisit time (16-day) that is small enough to acquire an adequate number of monthly images to represent the year.

More products are now becoming available (Sentinel-2, 5-day revisit time) that have a higher temporal

555 resolution, which would aid in the collection of more cloud free images to represent seasonality within the year.

Although it appears important to include seasonal land use dynamic, one may claim that the annual land-use implementation is enough when studying the effect of land use in hydrology. Our study shows a

significant impact of the representation of seasonal land-use in the SWAT+ model by reducing the errors

560 in water consumption estimations.

## 5. Conclusion

Understanding of the spatial-temporal variability of agricultural water consumption in terms of blue water, requires accurate estimates of ET. This study has demonstrated the importance of incorporating seasonal land-use dynamic to improve simulated ET for further blue and green ET estimates ~~in-using a~~

565 SWAT+ ~~model~~. Although the static representation gives ~~equally~~ reasonable ~~ey~~ good  $R^2$  results of more than

0.5, we found out that the RMSE for the static model result is significantly ~~higher~~ ~~as~~ compared to the RMSE of the dynamic ~~seasonal~~ model result by about 112 mm per year. Moreover, the ET from the dynamic SWAT+ model gave ~~a~~ low ~~a~~-PBIAS ~~ef~~(13%) and a ~~n~~ ~~relatively good~~ NSE of 0.4 compared to the ET from static SWAT+ that gives ~~a~~ higher PBIAS (20.8%) and a ~~very low~~~~negative~~ NSE of -0.46. The

570 study showed that a dynamic ~~land use~~ representation in the SWAT+ model gave ~~a closer comparison~~

~~to ET estimates closer to the~~ remote sensing ET ~~as~~ compared to the default model with a static land-use representation. The ~~improved ET maps with calculated blue water use~~ from the dynamic SWAT+ model

~~improved the blue ET estimates as compared to use of static ET maps that does not implement irrigation in dry season. Hence, estimated blue ET correspond to the known irrigated area and the calculated to the~~

575 blue ~~water ET~~ amount ~~is in line~~~~conforms with previous of past~~ ~~studies~~ ~~study done in the basin~~ (Msigwa et al., 2021). It is concluded that the representation of ~~seasonal~~ land use dynamics is essential to correctly

simulate the agricultural (blue and green) water consumption. Also, for land use change studies, it is

important to correctly represent the ~~seasonal~~ land use dynamics.

## References

580 Abiodun, O. O., Guan, H., Post, V. E. A., and Batelaan, O.: Comparison of MODIS and SWAT Evapotranspiration over a Complex Terrain at Different Spatial Scales, Hydrol. Earth Syst. Sci. Discuss., 1–36, <https://doi.org/10.5194/hess-2017-599>, 2017.

Alemayehu, T., van Griensven, A., and Bauwens, W.: Evaluating CFSR and WATCH data as input to SWAT for the estimation of the potential evapotranspiration in a data-scarce Eastern-African catchment, J. Hydrol. Eng., 21, 1–16,

585 [https://doi.org/10.1061/\(ASCE\)HE.1943-5584.0001305](https://doi.org/10.1061/(ASCE)HE.1943-5584.0001305), 2016.

Amri, R., Zribi, M., Lili-Chabaane, Z., Duchemin, B., Gruhier, C., and Chehbouni, A.: Analysis of vegetation behavior in a North African semi-arid region, Using SPOT-VEGETATION NDVI data, *Remote Sens.*, 3, 2568–2590, <https://doi.org/10.3390/rs3122568>, 2011.

Anderson, J. R., Hardy, E. E., Roach, J. T., Witmer, R. E., Anderson, B. J. R., Hardy, E. E., Roach, J. T., and Witmer, R. E.:  
590 A land use and land cover classification system for use with remote sensor data, 1976.

Anderson, M. C., Norman, J. M., Mecikalski, J. R., Otkin, J. A., and Kustas, W. P.: A climatological study of evapotranspiration and moisture stress across the continental United States based on thermal remote sensing: 2. Surface moisture climatology, *J. Geophys. Res.*, 112, 1–13, <https://doi.org/10.1029/2006JD007507>, 2007.

Arnold, J. G., Bieger, K., White, M. J., Srinivasan, R., Dunbar, J. A., and Allen, P. M.: Use of decision tables to simulate  
595 management in SWAT+, 10, 1–10, <https://doi.org/10.3390/w10060713>, 2018.

Bieger, K., Arnold, J. G., Rathjens, H., White, M. J., Bosch, D. D., Allen, P. M., Volk, M., and Srinivasan, R.: Introduction to SWAT+, A Completely Restructured Version of the Soil and Water Assessment Tool, *J. Am. Water Resour. Assoc.*, 53, 115–130, <https://doi.org/10.1111/1752-1688.12482>, 2017.

van Eekelen, M. W., Bastiaanssen, W. G. M., Jarmain, C., Jackson, B., Ferreira, F., van der Zaag, P., Saraiva Okello, A.,  
600 Bosch, J., Dye, P., Bastidas-Obando, E., Dost, R. J. J., and Luxemburg, W. M. J.: A novel approach to estimate direct and indirect water withdrawals from satellite measurements: A case study from the Incomati basin, *Agric. Ecosyst. Environ.*, 200, 126–142, <https://doi.org/10.1016/j.agee.2014.10.023>, 2015.

Falkenmark, M. and Rockström, J.: The new blue and green water paradigm: Breaking new ground for water resources planning and management, *J. Water Resour. Plan. Manag.*, 132, 129–132, [https://doi.org/10.1061/\(ASCE\)0733-9496\(2006\)132:3\(129\)](https://doi.org/10.1061/(ASCE)0733-9496(2006)132:3(129)), 2006.

605 FAO and IHE Delft: Water Accounting in the Litani River Basin-Remote sensing for water productivity, Water accounting series, Rome, 2019.

Feng, H., Zhao, X., Chen, F., and Wu, L.: Using land use change trajectories to quantify the effects of urbanization on urban heat island, *Adv. Sp. Res.*, 53, 463–473, <https://doi.org/10.1016/j.asr.2013.11.028>, 2014.

610 Ferreira, L. G., Yoshioka, H., Huete, A., and Sano, E. E.: Seasonal landscape and spectral vegetation index dynamics in the Brazilian Cerrado: An analysis within the Large-Scale Biosphere-Atmosphere Experiment in Amazonia (LBA), *Remote Sens. Environ.*, 87, 534–550, <https://doi.org/10.1016/j.rse.2002.09.003>, 2003.

Gao, J., Sheshukov, A. Y., Yen, H., Kastens, J. H., and Peterson, D. L.: Impacts of incorporating dominant crop rotation patterns as primary land use change on hydrologic model performance, *Agric. Ecosyst. Environ.*, 247, 33–42,  
615 <https://doi.org/10.1016/j.agee.2017.06.019>, 2017.

Gashaw, T., Tulu, T., Argaw, M., and Worqlul, A. W.: Modeling the hydrological impacts of land use/land cover changes in the Andassa watershed, Blue Nile Basin, Ethiopia, *Sci. Total Environ.*, 619–620, 1394–1408, <https://doi.org/10.1016/j.scitotenv.2017.11.191>, 2018.

Glavan, M. ˇ, Pintar, M., and Urbanc, J.: Spatial variation of crop rotations and their impacts on provisioning ecosystem services on the river Drava alluvial plain Sustainability of Water Quality and Ecology Spatial variation of crop rotations and their impacts on provisioning ecosystem services, *Sustain. Water Qual. Ecol.*, <https://doi.org/10.1016/j.swaqe.2015.01.004>, 2015.

van Griensven, A., Ndomba, P., Yalew, S., and Kilonzo, F.: Critical review of SWAT applications in the upper Nile basin countries, *Hydrol. Earth Syst. Sci.*, 16, 3371–3381, <https://doi.org/10.5194/hess-16-3371-2012>, 2012.

Guerschman, J. P., Van Dijk, A. I. J. M., Mattersdorf, G., Beringer, J., Hutley, L. B., Leuning, R., Pipunic, R. C., and Sherman, B. S.: Scaling of potential evapotranspiration with MODIS data reproduces flux observations and catchment water balance observations across Australia, *J. Hydrol.*, 369, 107–119, <https://doi.org/10.1016/j.jhydrol.2009.02.013>, 2009.

Hargreaves, G. H. and Samani, Z. A.: Estimating potential evapotranspiration, *J. Irrig. Drain. Eng.*, 108, 225–230, 1982.

Hengl, T., Heuvelink, G. B. M., Kempen, B., Leenaars, J. G. B., Walsh, M. G., Shepherd, K. D., Sila, A., MacMillan, R. A., De Jesus, J. M., Tamene, L., and Tondoh, J. E.: Mapping soil properties of Africa at 250 m resolution: Random forests significantly improve current predictions, *PLoS One*, 10, 1–26, <https://doi.org/10.1371/journal.pone.0125814>, 2015.

Hoekstra, A. Y.: Green-blue water accounting in a soil water balance, *Adv. Water Resour.*, 129, 112–117, <https://doi.org/10.1016/j.advwatres.2019.05.012>, 2019.

Hu, G. and Lia, L.: Monitoring of evapotranspiration in a semi-arid inland river basin by combining microwave and optical remote sensing observations, *Remote Sens.*, 7, 3056–3087, <https://doi.org/https://doi.org/10.3390/rs70303056>, 2015.

Hugo, V., Espinoza-dávalos, G. E., Hessels, T. M., Moreira, D. M., Comair, G. F., and Bastiaanssen, W. G. M.: The spatial variability of actual evapotranspiration across the Amazon River Basin based on remote sensing products validated with flux towers, *Ecol. Process. Process.*, 8, 2019.

IHE Delft: ET Ensemble Version 1.0 (ETensV1.0) Technical Documentation, 2020.

Jain, M., Mondal, P., Defries, R. S., Small, C., and Galford, G. L.: Remote Sensing of Environment Mapping cropping intensity of smallholder farms: A comparison of methods using multiple sensors, *Remote Sens. Environ.*, 134, 210–223, <https://doi.org/10.1016/j.rse.2013.02.029>, 2013.

Jeyrani, F., Morid, S., and Srinivasan, R.: Assessing basin blue–green available water components under different management and climate scenarios using SWAT, *Agric. Water Manag.*, 256, 107074, <https://doi.org/10.1016/j.agwat.2021.107074>, 2021.

Koch, F. J., Van Griensven, A., Uhlenbrook, S., Tekleab, S., and Teferi, E.: The effects of land use change on hydrological responses in the Choke Mountain Range (Ethiopia) - A new approach addressing land use dynamics in the model SWAT, *iEMSSs 2012 - Manag. Resour. a Ltd. Planet Proc. 6th Bienn. Meet. Int. Environ. Model. Softw. Soc.*, 3022–3029, 2012.

Liang, J., Liu, Q., Zhang, H., Li, X., Qian, Z., Lei, M., Li, X., Peng, Y., Li, S., and Zeng, G.: Interactive effects of climate variability and human activities on blue and green water scarcity in rapidly developing watershed, *J. Clean. Prod.*, 265, 121834, <https://doi.org/10.1016/j.jclepro.2020.121834>, 2020.

Liu, J. and Yang, H.: Spatially explicit assessment of global consumptive water uses in cropland: Green and blue water, *J. Hydrol.*, 384, 187–197, <https://doi.org/10.1016/j.jhydrol.2009.11.024>, 2010.

Mertens, B. and Lambin, E. F.: Land-Cover-Change Trajectories in Southern Cameroon, *Ann. Assoc. Am. Geogr.*, 90, 467–494, <https://doi.org/10.1111/0004-5608.00205>, 2000.

655 Miralles, D. G., Holmes, T. R. H., De Jeu, R. A. M., Gash, J. H., Meesters, A. G. C. A., and Dolman, A. J.: Global land-surface evaporation estimated from satellite-based observations, *Hydrol. Earth Syst. Sci.*, 15, 453–469, <https://doi.org/10.5194/hess-15-453-2011>, 2011.

Msigwa, A., Komakech, H. C., Verbeiren, B., Salvadore, E., Hessels, T., Weerasinghe, I., and van Griensven, A.: Accounting for seasonal land use dynamics to improve estimation of agricultural irrigation water withdrawals, 11, 660 <https://doi.org/10.3390/w11122471>, 2019.

Msigwa, A., Komakech, H. C., Salvadore, E., Seyoum, S., Mul, M. L., and Griensven, A. Van: Comparison of blue and green water fluxes for different land use classes in a semi-arid cultivated catchment using remote sensing, *J. Hydrol. Reg. Stud.*, 36, 100860, <https://doi.org/10.1016/j.ejrh.2021.100860>, 2021.

Mu, Q., Zhao, M., and Running, S. W.: Improvements to a MODIS global terrestrial evapotranspiration algorithm, *Remote Sens. Environ.*, 115, 1781–1800, <https://doi.org/10.1016/j.rse.2011.02.019>, 2011.

Ndomba, P., Mtalo, F., and Killingtveit, A.: SWAT model application in a data scarce tropical complex catchment in Tanzania, *Phys. Chem. Earth*, 33, 626–632, <https://doi.org/10.1016/j.pce.2008.06.013>, 2008.

Neitsch, S. L., Arnold, J. G., Kiniry, J. R., Srinivasan, R., and Williams, J. R.: Soil and Water Assessment Tool—User’s Manual 2002, TWRI Report TR-192, 412 pp., 2002.

670 Nkwasa, A., Chawanda, C. J., Msigwa, A., Komakech, H. C., Verbeiren, B., and van Griensven, A.: How can we represent seasonal land use dynamics in SWAT and SWAT+ models for African cultivated catchments, 12, 1–19, <https://doi.org/10.3390/W12061541>, 2020.

Notter, B., Hurni, H., Wiesmann, U., and Abbaspour, K. C.: Modelling water provision as an ecosystem service in a large East African river basin, *Hydrol. Earth Syst. Sci.*, 16, 69–86, <https://doi.org/10.5194/hess-16-69-2012>, 2012.

675 Schuol, J., Abbaspour, K. C., Yang, H., Srinivasan, R., and Zehnder, A. J. B.: Modeling blue and green water availability in Africa, *Water Resour. Res.*, 44, 1–18, <https://doi.org/10.1029/2007WR006609>, 2008.

Senay, G. B., Bohms, S., Singh, R. K., Gowda, P. H., Velpuri, N. M., Alemu, H., and Verdin, J. P.: Operational Evapotranspiration Mapping Using Remote Sensing and Weather Datasets: A New Parameterization for the SSEB Approach, *J. Am. Water Resour. Assoc.*, 49, 577–591, <https://doi.org/10.1111/jawr.12057>, 2013.

680 Senay, G. B., Friedrichs, M., Singh, R. K., Manohar, N., Velpuri, N. M., and Manohar, N.: Evaluating Landsat 8 evapotranspiration for water use mapping in the Colorado River Basin, *Remote Sens. Environ.*, 185, 171–185, <https://doi.org/10.1016/j.rse.2015.12.043>, 2016.

Serur, A. B.: Modeling blue and green water resources availability at the basin and sub-basin level under changing climate in the Weyb River basin in Ethiopia, *Sci. African*, 7, e00299, <https://doi.org/10.1016/j.sciaf.2020.e00299>, 2020.

685 Su, Z.: The Surface Energy Balance System ( SEBS ) for estimation of turbulent heat fluxes To cite this version : HAL Id : hal-00304651 The Surface Energy Balance System ( SEBS ) for estimation of turbulent heat fluxes, *Hydrol. Earth Syst. Sci.*

Discuss., 6, 85–100, 2002.

Swetnam, R. D.: Rural land use in England and Wales between 1930 and 1998: Mapping trajectories of change with a high resolution spatio-temporal dataset, Landsc. Urban Plan., 81, 91–103, <https://doi.org/10.1016/j.landurbplan.2006.10.013>, 2007.

690 Velpuri, N. M. and Senay, G. B.: Partitioning Evapotranspiration into Green and Blue Water Sources in the Conterminous United States, Scientific Reports, Springer US, 1–12 pp., <https://doi.org/10.1038/s41598-017-06359-w>, 2017.

Wagner, P. D., Bhallamudi, S. M., Narasimhan, B., Kantakumar, L. N., Sudheer, K. P., Kumar, S., Schneider, K., and Fiener, P.: Dynamic integration of land use changes in a hydrologic assessment of a rapidly developing Indian catchment, Sci. Total Environ., 539, 153–164, <https://doi.org/10.1016/j.scitotenv.2015.08.148>, 2016.

695 Wagner, P. D., Bhallamudi, S. M., Narasimhan, B., Kumar, S., Fohrer, N., and Fiener, P.: Comparing the effects of dynamic versus static representations of land use change in hydrologic impact assessments, Environ. Model. Softw., 122, 1–9, <https://doi.org/10.1016/j.envsoft.2017.06.023>, 2019.

Wang, D., Gong, J., Chen, L., Zhang, L., Song, Y., and Yue, Y.: Spatio-temporal pattern analysis of land use/cover change trajectories in Xihe watershed, Int. J. Appl. Earth Obs. Geoinf., 14, 12–21, <https://doi.org/10.1016/j.jag.2011.08.007>, 2012.

700 Woldesenbet, T. A., Elagib, N. A., Ribbe, L., and Heinrich, J.: Hydrological responses to land use/cover changes in the source region of the Upper Blue Nile Basin, Ethiopia, Sci. Total Environ., 575, 724–741, <https://doi.org/10.1016/j.scitotenv.2016.09.124>, 2017.

Xie, P., Zhuo, L., Yang, X., Huang, H., Gao, X., and Wu, P.: Spatial-temporal variations in blue and green water resources , water footprints and water scarcities in a large river basin : A case for the Yellow River basin, J. Hydrol., 590, 125222, <https://doi.org/10.1016/j.jhydrol.2020.125222>, 2020.

705 Zhou, Q., Li, B., and Kurban, A.: Trajectory analysis of land cover change in arid environment of China, Int. J. Remote Sens., 29, 1093–1107, <https://doi.org/10.1080/01431160701355256>, 2008.

Zomlot, Z., Verbeiren, B., Huysmans, M., and Batelaan, O.: Trajectory analysis of land use and land cover maps to improve spatial-temporal patterns, and impact assessment on groundwater recharge, J. Hydrol., <https://doi.org/10.1016/j.jhydrol.2017.09.032>, 2017.

## Appendices

### Appendix A. Make Management Script

```

import sys
715 from PIL import Image
import numpy as np

def open_tif_as_array(tif_file):
    im = Image.open(tif_file)
720    imarray = np.array(im)

```

```

    return imarray

def empty_line():
    print("")

725 def write_to(filename, text_to_write, report = False):
    """
    a function to write to file
    """
    730 g = open(filename, 'w')
    try:
        g.write(text_to_write)
        if report:
            print('\n\t> file saved to ' + filename)
    735 except:
        print("\t> error writing to {0}, make sure the file is not open in another program"
    .format(
        filename))
        response = input("\t> continue? (Y/N): ")
    740 if response == "N" or response == "n":
        sys.exit()
    g.close

def show_progress(count, end_val, string_before = "percent complete", string_after = "", ba
745 r_length = 30):
    percent = float(count) / end_val
    hashes = "#" * int(round(percent * bar_length))
    spaces = ' ' * (bar_length - len(hashes))
    sys.stdout.write("\r{str_b} [{bar}] {pct}% {str_after}\t\t".format(
    750 str_b = string_before,
        bar = hashes + spaces,
        pct = '{0:.2f}'.format(percent * 100),
        str_after = string_after))
    sys.stdout.flush()
755

def read_from(filename):
    """
    a function to read ascii files
    """
    760 try:
        g = open(filename, 'r')
    except:
        print("\t> error reading {0}, make sure the file exists".format(filename))
        return
    765 file_text = g.readlines()
    g.close
    return file_text

```

```

class schedule_data:
770     def __init__(self, crop_name):
        self.crop_name = crop_name
        self.oct_plant = ""
        self.oct_harvest = ""
        self.aug_plant = ""
775        self.aug_harvest = ""
        self.mar_plant = ""
        self.mar_harvest = ""

780 base_txt = "C:/Users/james/Desktop/root/anna/new/new_swat_plus_model/kikuletwa/Scenarios/De
fault/TxtInOut"
inputs_path = "trajectory_files"

# read trajectory data
785 trajectories = open_tif_as_array("{base}/{fn}".format(base = inputs_path, fn = "trajectory_
map_thres.tif"))
legend_raw = read_from("{base}/{fn}".format(base = inputs_path, fn = "trajectory_lookup_fn
al.csv"))
dates_raw = read_from("{base}/{fn}".format(base = inputs_path, fn = "crop_plant_harvest.csv
"))
790 landuse_lum_raw = """landuse.lum: created for trajectories
name           cal_group      plnt_com      mgt      cn
2           cons_prac      urban      urb_ro      ov_mann      tile
           sep           vfs           grww           bmp
595 """
plant_ini_raw = """plant.ini: created for trajectories
pcom_name      plt_cnt rot_yr_ini  plt_name  lc_status  lai_init      bm_init
phu_init      plnt_pop  yrs_init    rsd_init
595 """
800 management_raw = """management.sch: created for trajectories
name      numb_ops  numb_auto      op_typ      mon      day
hu_sch      op_data1  op_data2  op_data3
595 """
805 landuse_lum = landuse_lum_raw
plant_ini = plant_ini_raw

810 trajectories_dictionary = {}
# trajectory_hru_lum_dict = {}
crop_schedule_dictionary = {}
month_dictionary = {'None': "None", "Jan": "1", "Feb": "2", "Mar": "3", "Apr": "4", "May": "5",
"Jun": "6", "Jul": "7", "Aug": "8", "Sep": "9", "Oct": "10", "Nov": "11", "Dec": "12"}

815 for line in dates_raw[1:]:
    parts = line.split(",")

```

```

        crop_schedule_dictionary[parts[0].lower()] = schedule_data(parts[0])
        crop_schedule_dictionary[parts[0].lower()].oct_plant = "{0}".format(parts[5]).strip("\n")
820    ")
        crop_schedule_dictionary[parts[0].lower()].oct_harvest = "{0}".format(parts[6]).strip("\n")
        \n")
        crop_schedule_dictionary[parts[0].lower()].aug_plant = "{0}".format(parts[3]).strip("\n")
        ")
        crop_schedule_dictionary[parts[0].lower()].aug_harvest = "{0}".format(parts[4]).strip("\n")
825 \n")
        crop_schedule_dictionary[parts[0].lower()].mar_plant = "{0}".format(parts[1]).strip("\n")
        ")
        crop_schedule_dictionary[parts[0].lower()].mar_harvest = "{0}".format(parts[2]).strip("\n")
        \n")
830
for line in legend_raw[1:]:
    trajectories_dictionary[line.split(",")[1].lower()] = line.split(",")[2].strip("\n").lower()

835 growing_list = ["FRST", "BANA", "SHRB", "SUGC"]

for crop_name in trajectories_dictionary:
    # create lum
    parts = trajectories_dictionary[crop_name].split("-")
    com_mgt_prefix = "{0}_{1}_{2}".format(parts[0][:3], parts[1][:3], parts[2][:3])
    com_mgt_prefix = com_mgt_prefix.lower()
    if True: #not ((parts[0] == parts[1]) and (parts[0] == parts[2])):
        line_ = "{lum_t}           null           {plt_comm} {mgt}           rc_strow_g
840           cross_slope      null      null      convtill_nores      null
        null           null           null           null \n".format(
        lum_t = trajectories_dictionary[crop_name].lower().replace("-", "_"),
        plt_comm = "{0}_c".format(com_mgt_prefix),
        mgt = "{0}_m".format(com_mgt_prefix),
    )
    landuse_lum += line_
    # print(trajectories_dictionary[crop_name])

    # create comm
    comm_ = "{comm_n}_c           /no           1 \n".format(comm_n = com_mgt_prefix)
845    plt_count = 0
    done = []
    for plt in parts:
        if plt == "AGRL":
            for agrl_crop in ["TOMA", "CORN", "SOYB"]:
850            if not agrl_crop.lower() in done:
                if plt in growing_list:
                    grow_ini = "y"
                else:
                    grow_ini = "n"
855            plt_count += 1

```



```

915         agrl_list = ["corn"]

920             if parts[plant_index] == "agrl":
921                 for agrl_crop_mgt in agrl_list:
922                     if plant_index == 0:
923                         date_day_plant = crop_schedule_dictionary[agrl_crop_mgt].mar_plant.split(
924                             t("-")[-1])
925                         date_mnt_plant = crop_schedule_dictionary[agrl_crop_mgt].mar_plant.split(
926                             t("-")[-1])
927                         if plant_index == 1:
928                             date_day_plant = crop_schedule_dictionary[agrl_crop_mgt].aug_plant.split(
929                             t("-")[-1])
930                         date_mnt_plant = crop_schedule_dictionary[agrl_crop_mgt].aug_plant.split(
931                             t("-")[-1])
932                         if plant_index == 2:
933                             date_day_plant = crop_schedule_dictionary[agrl_crop_mgt].oct_plant.split(
934                             t("-")[-1])
935                         date_mnt_plant = crop_schedule_dictionary[agrl_crop_mgt].oct_plant.split(
936                             t("-")[-1])

937                         management_body_line = "
938                             {activity}{mnt}{day}          0.00000           {crp}           null      {ord
939                             er}.00000  ".format(
940                                 activity = "plnt",
941                                 mnt = month_dictionary[date_mnt_plant].strip(" ").rjust(10),
942                                 day = date_day_plant.rjust(10),
943                                 crp = agrl_crop_mgt.lower(),
944                                 order = counter_mgt,
945                                 )
946                         management_section_body += "{0}\n".format(management_body_line)
947                         counter_mgt += 1
948                         for agrl_crop_mgt in agrl_list:
949                             if plant_index == 0:
950                                 date_day_harvest = crop_schedule_dictionary[agrl_crop_mgt].mar_harvest.
951                                 split("-")[-1]
952                                 date_mnt_harvest = crop_schedule_dictionary[agrl_crop_mgt].mar_harvest.
953                                 split("-")[-1]
954                                 if plant_index == 1:
955                                     date_day_harvest = crop_schedule_dictionary[agrl_crop_mgt].aug_harvest.
956                                     date_mnt_harvest = crop_schedule_dictionary[agrl_crop_mgt].aug_harvest.
957                                     split("-")[-1]
958                                     if plant_index == 2:
959                                         date_day_harvest = crop_schedule_dictionary[agrl_crop_mgt].oct_harvest.
960                                         date_mnt_harvest = crop_schedule_dictionary[agrl_crop_mgt].oct_harvest.
961                                         split("-")[-1]

```

```

    management_body_line = "
{activity}{mnt}{day}      0.00000           {crp}           null      {ord
965 er}.00000 ".format(
        activity = "hvkl",
        mnt = month_dictionary[date_mnt_harvest].strip(" ").rjust(10),
        day = date_day_harvest.rjust(10),
        crp = agr1_crop_mgt.lower(),
        order = counter_mgt,
    )
    management_section_body += "{0}\n".format(management_body_line)
    counter_mgt += 1

975
    elif parts[plant_index] in crop_schedule_dictionary:
        if not parts[plant_index] == "past":

            if plant_index == 0:
                date_day_plant = crop_schedule_dictionary[parts[plant_index]].mar_plant
980 .split("-")[0]
                date_mnt_plant = crop_schedule_dictionary[parts[plant_index]].mar_plant
                .split("-")[1]
            if plant_index == 1:
                date_day_plant = crop_schedule_dictionary[parts[plant_index]].aug_plant
985 .split("-")[0]
                date_mnt_plant = crop_schedule_dictionary[parts[plant_index]].aug_plant
                .split("-")[1]
            if plant_index == 2:
                date_day_plant = crop_schedule_dictionary[parts[plant_index]].oct_plant
990 .split("-")[0]
                date_mnt_plant = crop_schedule_dictionary[parts[plant_index]].oct_plant
                .split("-")[1]

                management_body_line = "
995     {activity}{mnt}{day}      0.00000           {crp}           null      {ord
er}.00000 ".format(
        activity = "plnt",
        mnt = month_dictionary[date_mnt_plant].strip(" ").rjust(10),
        day = date_day_plant.rjust(10),
        crp = parts[plant_index].lower(),
        order = counter_mgt,
    )
    management_section_body += "{0}\n".format(management_body_line)
    counter_mgt += 1

1000
1005
        if plant_index == 0:
            date_day_harvest = crop_schedule_dictionary[parts[plant_index]].mar_har
vest.split("-")[0]
            date_mnt_harvest = crop_schedule_dictionary[parts[plant_index]].mar_har
1010 vest.split("-")[1]

```

```

    if plant_index == 1:
        date_day_harvest = crop_schedule_dictionary[parts[plant_index]].aug_har
vest.split("-")[0]
        date_mnt_harvest = crop_schedule_dictionary[parts[plant_index]].aug_har
1015 vest.split("-")[1]
        if plant_index == 2:
            date_day_harvest = crop_schedule_dictionary[parts[plant_index]].oct_har
vest.split("-")[0]
            date_mnt_harvest = crop_schedule_dictionary[parts[plant_index]].oct_har
1020 vest.split("-")[1]

            management_body_line =
{activity}{mnt}{day} 0.00000 {crp} null {ord
er}.00000 ".format(
1025
            activity = "hvkl",
            mnt = month_dictionary[date_mnt_harvest].strip(" ").rjust(10),
            day = date_day_harvest.rjust(10),
            crp = parts[plant_index].lower(),
            order = counter_mgt,
)
            management_section_body += "{0}\n".format(management_body_line)
            counter_mgt += 1

        if counter_mgt == 0:
            continue
1035

        management_raw += management_section_head.format(mgt_name = schedule_name, number_manua
l = counter_mgt, number_auto = number_of_auto_ops) + "\n" + management_section_body
1040 # fix hrus based on dictionary

        hru_data_string = """hru-data.hru: for trajectories
        id name topo hydro soil
        lu_mgt soil_plant_init surf_stor snow field
"""
1045

        hru_data_hru_raw = read_from("{base}/{fn}".format(base = base_txt, fn = "hru-data.hru"))

        for line in hru_data_hru_raw[2:]:
            for_part = line
            for i in range(0, 20):
                for_part = for_part.replace(" ", " ")
            parts = for_part.split(" ")
            # print(parts[6].split("_")[0])
1050            hru_data_string += line.replace(parts[6], trajectories_dictionary[parts[6].split("_")[0]].lower().replace("-", "_"))

        write_to("{base}/{fn}".format(base = 'model_files\Scenarios\Default\TxtInOut', fn = "landus
e.lum"), landuse_lum)

```

```

1060 write_to("{base}/{fn}".format(base = 'model_files\Scenarios\Default\TxtInOut', fn = "management.sch"), management_raw)
write_to("{base}/{fn}".format(base = 'model_files\Scenarios\Default\TxtInOut', fn = "plant.ini"), plant_ini)
write_to("{base}/{fn}".format(base = 'model_files\Scenarios\Default\TxtInOut', fn = "hru-data.hru"), hru_data_string)
1065

```

1070

1075

## Appendix B. Trajectories Description

1080 **Table 1B.** Trajectories [examples](#) for each fake land-use code use for dynamic SWAT+ implementation.

Map_id	Code	Trajectory
1	TUWO	TUWO-TUWO-TUWO
2	GRAS	GRAS-GRAS-GRAS
6	BSVG	BSVG-BSVG-BSVG
11	FRST	FRST-FRST-FRST
78	BANA	BANA-BANA-BANA
110	HMEL	SHRB-SHRB-SHRB
121	INDN	CORN-BSVG-BSVG
146	LETT	CORN-BSVG-PAST
167	PAST	PAST-PAST-PAST
182	SUGC	SUGC-SUGC-SUGC
204	ASPN	FRST-BSVG-FRST
224	LIMA	CORN-PAST-PAST
225	MAPL	CORN-PAST-BSVG
243	MESQ	CORN- <a href="#">AGRLTOMA</a> -PAST
248	MIGS	CORN- <a href="#">AGRLTOMA</a> -BSVG
249	MINT	<a href="#">AGRLTOMA</a> - <a href="#">AGRLTOMA</a> -BSVG
254	MIXC	CORN- <a href="#">AGRLTOMA</a> - <a href="#">AGRLTOMA</a>

**Table 2B.** Dynamic agricultural land-use trajectory and their crop or vegetation cover meaning

ID	Trajectory	Crop/vegetation cover Meaning
1	CORN-PAST-PAST	rainfed maize-grass-grass
2	CORN-PAST-BSVG	rainfed maize-grass- sparse vegetation
3	CORN- <u>AGRLTOMA</u> -PAST	rainfed maize- tomato-grass
4	CORN- <u>AGRLTOMA</u> -BSVG	rainfed maize-tomato-sparse vegetation
5	AGRL- <u>AGRLTOMA</u> -BSVG	Beans-tomato-sparse vegetation
6	CORN- <u>AGRLTOMA</u> - <u>AGRLIRRM</u>	rainfed maize-tomato-irrigated maize
7	CORN-PAST- <u>IRRMAAGRL</u>	Rainfed maize-grass-irrigated maize

**Table 3B. Land use classes as represented in the Static SWAT+ Model**

<u>LANDUSE_ID</u>	<u>Land use Class</u>	<u>SWAT_CODE</u>
<u>1</u>	<u>Water</u>	<u>WATR</u>
<u>2</u>	<u>Grazed grassland</u>	<u>PAST</u>
<u>3</u>	<u>Grazed shrubland</u>	<u>CRGR</u>
<u>4</u>	<u>Space vegetation</u>	<u>BSVG</u>
<u>5</u>	<u>Rainfed Maize</u>	<u>CORN</u>
<u>6</u>	<u>Irrigated Sugarcane</u>	<u>SUGC</u>
<u>7</u>	<u>Dense forest</u>	<u>FRST</u>
<u>8</u>	<u>Sub_Alpine grassland</u>	<u>GRAS</u>
<u>9</u>	<u>Woodland</u>	<u>TUWO</u>
<u>10</u>	<u>Mixed Crops</u>	<u>TOMAAGRL</u>
<u>11</u>	<u>Irrigated Banana and Coffee</u>	<u>BANA</u>
<u>12</u>	<u>Wetland</u>	<u>WEHB</u>
<u>13</u>	<u>Urban</u>	<u>URMD</u>
<u>14</u>	<u>Shrubland</u>	<u>SHRB</u>

## Appendix C. Data used in this study

1090 **Table 1C.** Summary of the different data used in the study with description and sources

Data Type	Description	Source/ reference
Climate	Ten station data of rainfall and four stations of maximum/minimum temperature	Tanzania Meteorological Agency (TMA) and Pangani Basin Water Office (PBWO)
Digital Elevation Model (DEM)	Elevation data from at 90m resolution	United States Geological Survey (USGS) website
Seasonal land use maps	Seasonal land use maps at 30m	(Msigwa et al., 2019)
Soil	Africa Soil Information System (AFSIS) at 250m resolution	(Hengl et al., 2015)
Remotely sensed based Actual ET	Ensemble ET from six remote sensing products	(IHE Delft, 2020)
Land management data	Planting dates, harvesting dates and irrigation application dates and frequency	Farmers interview